Author Query Form

Dear Author,

Below are the queries associated with your article; please answer all of these queries before sending the proof back to JAND.

Article checklist: In order to ensure greater accuracy, please check the following and make all necessary corrections before returning your proof.

1. Is the title of your article accurate and spelled correctly?
2. Please check affiliations including spelling, completeness, and correct linking to authors.
3. Did you remember to include acknowledgment of funding, if required, and is it accurate?

Query	Details Required	Author's Response
AQ1	Please check that the author names are in the proper order and spelled correctly. Also, please ensure that each author's given and surnames have been correctly identified	
AQ2	Please check address information	
AQ3	Please check and make sure page number for each paper in reference is listed rather than only the first page number	
AQ4	Please check and make sure journal names are fully spelled out in the references	

Dear Author,

Here are the proofs of your article.

- You can submit your corrections **online**, via **e-mail** or by **fax**.
- For **online** submission please insert your corrections in the online correction form. Always indicate the line number to which the correction refers.
- You can also insert your corrections in the proof PDF and **email** the annotated PDF.
- For fax submission, please ensure that your corrections are clearly legible. Use a fine black pen and write the correction in the margin, not too close to the edge of the page.
- Remember to note the **journal title**, **article number**, and **your name** when sending your response via e-mail or fax.
- **Check** the metadata sheet to make sure that the header information, especially author names and the corresponding affiliations are correctly shown.
- **Check** the questions that may have arisen during copy editing and insert your answers/ corrections.
- **Check** that the text is complete and that all figures, tables and their legends are included. Also check the accuracy of special characters, equations, and electronic supplementary material if applicable. If necessary refer to the *Edited manuscript.*
- The publication of inaccurate data such as dosages and units can have serious consequences. Please take particular care that all such details are correct.
- Please **do not** make changes that involve only matters of style. We have generally introduced forms that follow the journal's style.
  Substantial changes in content, e.g., new results, corrected values, title and authorship are not allowed without the approval of the responsible editor. In such a case, please contact the Editorial Office and return his/her consent together with the proof.
- If we do not receive your corrections **within 48 hours**, we will send you a reminder.
- Your article will be published **Online First** approximately one week after receipt of your corrected proofs. This is the **official first publication** citable with the DOI. **Further changes are, therefore, not possible.**
- The **printed version** will follow in a forthcoming issue.

Please note

After online publication, subscribers (personal/institutional) to this journal will have access to the complete article via the DOI using the URL: http://dx.doi.org/[DOI].
If you would like to know when your article has been published online, take advantage of our free alert service. For registration and further information go to: https://www.lhscientificpublishing.com/.

Due to the electronic nature of the procedure, the manuscript and the original figures will only be returned to you on special request. When you return your corrections, please inform us if you would like to have these documents returned.

Journal of Applied Nonlinear Dynamics 14(3) (2025) 719-743

Journal of Applied Nonlinear Dynamics

https://lhscientificpublishing.com/Journals/JAND-Default.aspx

Dynamic Interactions in Intraguild Predation: A Ratio-Dependent Model with Time Delay and Prey Refuge

S. Magudeeswaran[1], S. Vinoth[2†], R. Vadivel[3], Nallappan Gunasekaran[4]

[1] Department of Mathematics, Sree Saraswathi Thyagaraja College, Pollachi, 642 107, Tamilnadu, India
[2] Center for Nonlinear and Complex Networks, SRM Institute of Science and Technology, Ramapuram, Chennai, 600089, Tamilnadu, India
[3] Department of Mathematics, Faculty of Science and Technology, Phuket Rajabhat University, Phuket, 83000, Thailand
[4] Eastern Michigan Joint College of Engineering, Beibu Gulf University, Qinzhou, 535011, P. R. China

Submission Info

Communicated by Igor Franovic
Received 13 February 2024
Accepted 24 November 2024
Available online 1 July 2025

Keywords

Local stability
Hopf-bifurcation
Prey-predator
Time delay

Abstract

In this work, we propose a ratio-dependent intraguild predation model that incorporates fear and gestation delay. Further, the cost of the intraguild predator's fear is thought to decrease the size of the intraguild prey. The interaction between prey and predator takes place in the form ratio-dependence type. This type of functional response offers a valuable perspective by considering the feeding rates based on the relative abundance of both prey and predators. We first determine the conditions under which positive equilibrium points exist, and then we examine the local stability properties of the equilibria. In order to gain insight into the rich dynamics of the proposed non-delayed model, the occurrence of Hopf-bifurcation with respect to the fear parameter near the interior equilibrium point is discussed. Furthermore, we evaluate the local stability and the possibility of a Hopf bifurcation for the delayed model. The direction and stability of the Hopf bifurcation are also studied using the center manifold theorem. Finally, we conduct the numerical simulations to demonstrate our analytical results.

1 Introduction

Malthus [1] presented the first theory of population dynamics near the close of the eighteenth century. It is considered that the rate of population growth is directly related to the size of the existing population. This theory is called the "Malthusian theory of population". However, in a real situation, the unbounded solutions could not make the right prediction. Later, the logistical development model was established, defining natural controls for development as a result of restricted resources and area. Lotka and Volterra showed that the population model for the interaction of two species can be represented by a set of

†Corresponding author.
Email address: svinothappu@gmail.com

ISSN 2164-6457, eISSN 2164-6473/$-see front materials
DOI:10.5890/JAND.2025.09.014

nonlinear ordinary differential equations [2]. The existence of periodic solutions is also a feature of those equations. Functional response is a crucial term in the interaction between prey and predator, which indicates the prey consumption rate of predators, making the model more realistic from an ecological standpoint. Numerous studies have been conducted by choosing various functional responses, such as, Holling [3–5], Beddington-DeAngelis [6], Crowley-Martin [7, 8], and ratio-dependent [9–11] to observe their impact on various prey-predator models over the past few centuries. The feeding rate of predators depends not only on the density of prey but also on the proportion of predators; this is called the "ratio-dependent" functional response. It has been first introduced by [9]. Recently, many authors started to analyze the prey-predator model with ratio-dependent functional response. The qualitative behavior of the prey-predator model was investigated in [12], where they investigated the stability and Hopf-bifurcation for the diffusive prey-predator model with ratio-dependent functional response. The authors in [13] investigated the mathematical analysis for the prey-predator model with Allee effect in prey and ratio-dependent functional response.

Furthermore, the Lotka-Volterra model has been modified to take into account different ecological factors such as the Allee effect, stage structure, gestation delay, etc., and explore local and global behaviors. Due to the ease of observation, predation occurrences can be observed in the forest provinces where the prey-predator system has traditionally been thought to work by the predators directly affecting the prey population. However, according to current studies, predators affect the prey population not only by direct killing but also by instilling fear in prey populations, which affects the reproduction rate of the prey population. It was introduced by [14]. Prey populations are often wary of entering an open environment because of the fear instilled by predators, so they lack a free zone for performing routine behaviors like mating. Therefore, prey populations can be kept in check by the fear of predators. As a result, the cost of fear in the form of decreased reproduction must be taken into account. Recently, many researchers have begun to study the ecological model and its impact on fear. In [15], the authors investigated the presence of fear in predator-prey models with linear or Holling type II functional responses. They concluded that in the scenario of the linear type, the impact of fear has little effect on the characteristics of model dynamics. Whereas in the context of Holling type-II, the presence of fear has considerable consequences for predator-prey interaction. The authors in [16] investigated an intraguild predation model in the presence of fear and found that the strength of fear stabilized the system from chaotic behavior. They also discovered that fear can generate several stable limit cycles. Intraguild predation refers to ecological circumstances in which species interact as both predators and prey competing for shared resources. Beyond standard predator-prey models, modelling such interactions provides insights into the complex dynamics of species coexistence and population growth.

Due to conditions such as environmental deterioration, over-predation, widespread harvesting, over-exploitation, etc., many species have disappeared, and many more are on the edge of going extinct. Combining mathematical representations of diverse ecological systems with suitable actions is necessary, such as enhancing the conditions of their natural surroundings, curbing species interaction with outside factors that cause a decrease in their size, enforcing harvesting restrictions, constructing natural reserves, establishing conservation areas, and so on, to prevent species extinction and thus preserve our food chain. The term "prey refuge" is a fantastic idea for reducing the possibility of too much predation on prey populations. Prey hiding behavior may help to maintain predator-prey dynamics and protect prey refuges from predation. In biology and ecology, a species can defend itself from predators by concealing itself in a place that is isolated or inaccessible to predation. This act is called a refuge. The existence of refuges plays a crucial role in the survival of prey and predators. For instance, the impact of prey refuge in the stage-structured predator-prey model discussed in [17] and diffusive predator prey model examined in [18]. Also, the author found that the considered model predicts that when refuge usage is high enough, mature prey populations achieve their environmental carrying limit and predators

become extinct. The prey-predator model with harvesting and the effect of prey refuge were studied in [19]. They showed that when the predator becomes extinct, increasing the harvesting level for prey can decrease the density of prey population. The authors in [6] examined a prey-predator model with Beddington-DeAngelis functional response and prey refuge, and they performed a stability analysis to understand the system's dynamical behavior. In [20], the authors investigated the impact of the fear effect and prey refuge on the prey-predator model in fractional order. Stability and bifurcation analysis for the predator-prey model with square-root-type interactions were discussed in [21].

In a broad sense, it's possible that there's a time lag in the predator-prey system, which might affect the system's stability. Every biological event that occurs has a time delay. In nature, delayed models are more realistic. Delay differential equations exhibit significantly more complicated behaviour than ordinary differential equations. In the prey-predator system, the effect that causes prey to be digested within the predator population does not occur quickly. As a result, there is a time delay due to gestation. The two species of prey-predator model that incorporated the effects of delay and harvesting were investigated [22]. The authors in [23] studied the dynamical behavior of a time-delayed ratio-dependent predator-prey model with a predator stage structure. In [24], the authors analyzed the stability properties and the occurrence of bifurcation behavior for the fractional order predator-prey model with time delay. In [25], the authors used the comparison theorem, differential inequalities, and a new analysis method to explore a Lotka-Volterra ratio-dependent predator-prey model with delays and feedback controls.

In the following ways, our model differs from the model examined in earlier research.

(1) In [11], the ratio-dependent intraguild predator prey model with time delay is considered and the aim was to investigate the role of ratio-dependent functional response and time delay in terms of stability and Hopf bifurcation.

(2) The impacts of fear and refuge in a three-species Gause-type food chain model with hunting cooperation are considered in [26]. The combined effects of fear, refuge, cooperation, and harvesting in the two-species predator-prey model are examined in [27]. The predator-prey model with the combined effects of fear, refuge, and additional food with Crowley-Martin type interaction has been explored in [28]. In [29], the effect of fear and time delay are considered in an intraguild predation model.

(3) In the present work, we study the combined effects of fear, prey refuge and gestation time delay in an intraguild predator prey model. We also focus on the properties of the Hopf bifurcation which is not considered in [11, 29].

The following is the outline for the paper: The background, motivations, and objectives of this work are provided in Section 1. Section 2 discusses the existence of positive equilibrium points and their local stability analysis, as well as the requirement for the occurrence of Hopf-bifurcation in the non-delayed model. Section 3 deals with the delayed model's local stability and Hopf bifurcation analysis. Also, the direction and stability of Hopf bifurcation is discussed with the help of center manifold theorem. Sections 4 and 5 deal with numerical simulations and the conclusion, respectively.

2 Model without time delay

The goal of this section is to explore the intraguild predation model, which was described in [11] by considering ratio-dependent type functional response is of the from:

$$\begin{aligned}
\frac{dx}{dt} &= r_1 x(1-\frac{x}{pz}) - \frac{\alpha xy}{nx+y},\\
\frac{dy}{dt} &= r_2 y(1-\frac{y}{qz}) + \frac{\beta xy}{nx+y},\\
\frac{dz}{dt} &= z(\gamma - \delta x - \eta y),
\end{aligned} \tag{1}$$

with subject to the initial conditions are $x(0) = x_0 > 0,\ y(0) = y_0 > 0$, and $z(0) = z_0 > 0$, where

- x, y, and z represents the size of prey, predator and biotic resources at time t, respectively.
- $r_1, p, \alpha, r_2, q, \beta, \gamma, \delta$, and η are the positive parameters.
- r_1 and r_2 represent the growth rates of the prey and predator populations, respectively.
- The terms pz and qz are the ecological carrying capacities of the populations of intraguild prey and intraguild predator, respectively.
- The carrying capacity of each individual, intraguild prey and intraguild predator, are represented by the parameters p and q. We assume $0 < p < 1$ and $0 < q < 1$ with $p + q = 1$, therefore the total carrying capacity is $(p+q)z$. If q is greater than p, the intraguild prey population receives a greater proportion of the biological resources, resulting in a higher carrying capacity. That is, intraguild prey has the ability to grow larger than intraguild predators.
- The biotic resources' growth rate is γ, the rate of absorption of resources by intraguild prey is δxz, and the absorption rate of resources by intraguild predator is ηyz, where δ and η are the positive constants.
- The parameters α and β be denote the capturing rate and conversion rate of devoured intraguild prey to intraguild predator, respectively.

The following assumptions are made:

The decreasing function $H(k,y) = \frac{1}{1+ky}$ is incorporated into the prey growth to model the effect of fear in the prey population, where k represents the strength of fear due to the presence of a predator. In ratio-dependent functional response $\frac{xy}{nx+y}$, when resources are low relative to population density, the predator's per capita growth should decline with its density. The term $H(k,y)$ satisfies the below requirements [15].

$$H(0,y) = 1, H(k,0) = 1, \lim_{k\to\infty} = 0, \lim_{y\to\infty} = 0,$$

$$\frac{\partial H(k,y)}{\partial k} < 0, \frac{\partial H(k,y)}{\partial y} < 0.$$

We now separate the prey population into two classifications: protected populations that are off-limits to predators and open access populations that are liable to predation. It is referred to as prey refuge. Let μx be denotes the size of reserved prey population and $(1-\mu)x$ be the size of available prey species for predation. As a result, we alter the ratio-dependent functional response by considering the prey refuge's impact as follows: $f(x,y) = \frac{(1-\mu)xy}{(1-\mu)nx+y}$, where, n is the half saturation constant for intraguild prey

We extend the ratio-dependent model (1) by incorporating the impact of fear in the prey population and prey refuge. Hence, we can rewrite the model (1) in the form:

$$\begin{aligned}
\frac{dx}{dt} &= \frac{r_1 x}{1+ky}\left(1 - \frac{x}{pz}\right) - \frac{\alpha(1-\mu)xy}{(1-\mu)nx+y}, \\
\frac{dy}{dt} &= r_2 y\left(1 - \frac{y}{qz}\right) + \frac{\beta(1-\mu)xy}{(1-\mu)nx+y}, \\
\frac{dz}{dt} &= z(\gamma - \delta x - \eta y),
\end{aligned} \tag{2}$$

with subject to the initial conditions are $x(0) = x_0 > 0,\ y(0) = y_0 > 0$, and $z(0) = z_0 > 0$.

2.1 Existence of equilibrium points

It is easy to determine the positive equilibrium points for the model (2) and then examine the local stability of the obtained equilibria.

1. The prey free equilibrium $E_1(0, \frac{\gamma}{\eta}, \frac{\gamma}{\eta q})$.
2. The predator free equilibrium $E_2(\frac{\gamma}{\delta}, 0, \frac{\gamma}{\delta p})$.
3. The coexisting equilibrium $E^*(x^*, y^*, z^*)$, where

$$y^* = \frac{\gamma - \delta x^*}{\eta},$$
$$z^* = \frac{r_2(1-\mu)nx^*(\gamma-\delta x^*)\eta + r_2(\gamma^2 + \delta^2 x^{*2} - 2\gamma\delta x^*)}{r_2 q(1-\mu)n\eta^2 x^* + r_2 q(\gamma-\delta x^*)\eta + \beta(1-\mu)q\eta^2 x^*},$$

and solve following equation to get x^*,

$$M_1 x^{*4} + M_2 x^{*3} + M_3 x^{*2} + M_4 x^* + M_5 = 0, \tag{3}$$

where,

$$\begin{aligned}
M_1 =& \ \alpha(1-\mu)^2 kp\delta^3 r_2 n\eta - \alpha(1-\mu)kp\delta^4 r_2,\\
M_2 =& \ r_1 r_2 q\delta(1-\mu)n\eta^3 - r_1 r_2 q\delta\eta^2 + r_1\delta\beta(1-\mu)\eta^3 q - 2\alpha(1-\mu)^2 r_2 nk\delta^2\eta + \alpha(1-\mu)k2\gamma\delta^3\\
&- \alpha(1-\mu)^2 p\delta^2\eta^2 nr_2 + r_2\alpha(1-\mu)p\delta^3\eta - \alpha(1-\mu)^2 kp\delta^2 r_2 n\gamma\eta + 2\alpha(1-\mu)kp\gamma\delta^3,\\
M_3 =& \ -r_1 r_2\gamma\eta^3 qn(1-\mu) + r_1 r_2\gamma\eta^2 q\delta - r_1\gamma\eta^3\beta(1-\mu)q + r_1 r_2\delta\gamma q\eta^2 + 2\alpha(1-\mu)^2 k\gamma^2 r_2 n\eta\\
&- 4\gamma^2\delta^2\alpha(1-\mu)kr_2 + \alpha(1-\mu)^2 p\delta\eta^2 r_2 n\gamma - 2\alpha(1-\mu)p\delta^2\gamma\eta r_2 + \alpha(1-\mu)^2 r_2 np\gamma\eta^2\delta\\
&- \alpha(1-\mu)p\gamma\delta^3 r_2\eta + \alpha(1-\mu)^2 kpr_2 n\gamma^2\eta\delta - \alpha(1-\mu)kp\gamma^2\delta^2 r_- \alpha(1-\mu)kp\delta^2 r_2\gamma^2,\\
M_4 =& \ 2\alpha(1-\mu)k\gamma^3 r_2\delta + \alpha(1-\mu)p\delta\eta r_2\gamma^2 - \alpha r_2(1-\mu)^2 pn\gamma^2\eta^2\\
&+ 2\alpha(1-\mu)p\gamma^2\delta\eta r_2 - \alpha(1-\mu)^2 nkp\gamma^3 r_2\eta + 2\alpha(1-\mu)kp\gamma^3\delta,\\
M_5 =& \ -\left(r_1\gamma^2 r_2 q\eta^2 + \alpha(1-\mu)p\gamma^3\eta r_2 + \alpha(1-\mu)kp\gamma^4 r_2\right).
\end{aligned}$$

It is important to note that it is hard to express condition for number of the positive roots of Eq. (3) analytically. Therefore, the roots of Eq. (3) can be obtained by numerically. Assuming Eq. (3) has at least one positive x^*, then $E^*(x^*, y^*, z^*)$ is the coexisting equilibrium of the model (2) and also satisfies $\gamma > \delta x^*$. Where the E_2 always exists, further the existence of coexistence equilibrium E^* and E_1 is clearly depicted in Fig.2. The existence of equilibria is clearly shown numerically with help of nullcline plane in Fig.1. Where the existence of coexistence equilibrium E^* in two parameter plane is clearly depicted in Fig.2.

2.2 Local stability analysis

The long-term coexistence of species can analyzed with the help of the local stability property of the equilibrium points. The model's variational matrix is now calculated to examine the local stability properties for the model (2) at an arbitrarily chosen equilibrium point $E(x, y, z)$, denoted by

$$J(x,y,z) = \begin{bmatrix} \hat{a}_{11} & \hat{a}_{12} & \hat{a}_{13} \\ \hat{a}_{21} & \hat{a}_{22} & \hat{a}_{23} \\ \hat{a}_{31} & \hat{a}_{32} & \hat{a}_{33} \end{bmatrix}, \tag{4}$$

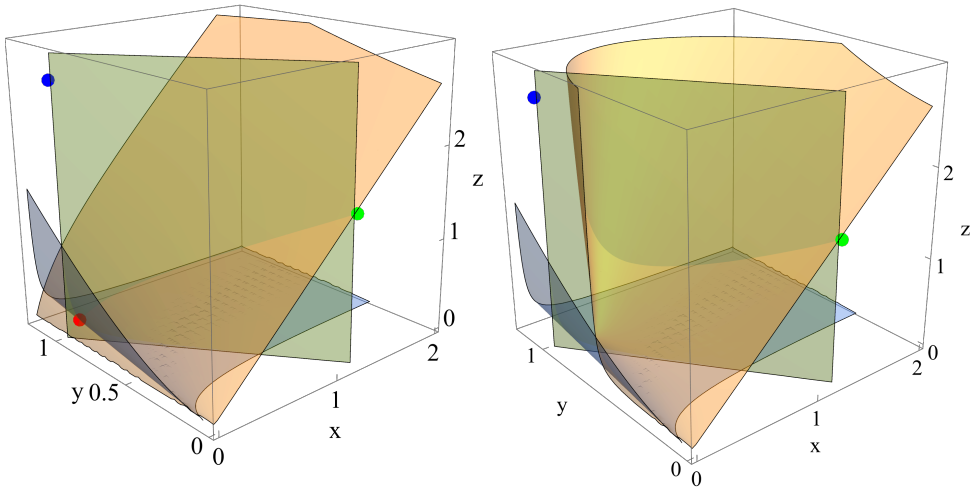

Fig. 1 (a) The nullcline plane for the model (2) has equilibria $E_1(0,0.960159,2.7355)$ (blue), $E_2(1.199,0,1.56733)$ (green), $E^*(0.0672843,0.906278,0.223604)$ (red) with $r_1 = 1.01$, $r_2 = 0.0031$, $\gamma = 2.41$, $\delta = 2.01$, $\eta = 2.51$, $p = 0.765$, $q = 0.351$, $\beta = 0.568$, $\alpha = 0.58$, $n = 1.71$, $\mu = 0.14$ and $k = 0.4$. (b) The nullcline plane for the model (2) has equilibria $E_1(0,0.960159,2.7355)$ (blue), $E_2(1.199,0,1.56733)$ (green), with $\mu = 0.1$, $k = 1.5$ and all other values are same as in (a).

where

$$\hat{a}_{11} = \frac{r_1}{1+ky} - \frac{2r_1x}{(1+ky)pz} - \frac{\alpha(1-\mu)y^2}{(n(1-\mu)x+y)^2},\ \hat{a}_{12} = \frac{r_1kx^2}{(1+ky)^2pz} - \frac{r_1kx}{(1+ky)^2} - \frac{\alpha(1-\mu)^2nx^2}{((1-\mu)nx+y)^2},$$
$$\hat{a}_{13} = \frac{r_1x^2}{(1+ky)pz^2},\ \hat{a}_{21} = \frac{\beta(1-\mu)y^2}{((1-\mu)nx+y)^2},\ \hat{a}_{22} = r_2 - \frac{2r_2y}{qz} + \frac{\beta(1-\mu)^2nx^2}{((1-\mu)nx+y)^2},$$
$$\hat{a}_{23} = \frac{r_2y^2}{qz^2},\ \hat{a}_{31} = -\delta x,\ \hat{a}_{32} = -\eta z,\ \hat{a}_{33} = \gamma - \eta z - \delta x.$$

Further, we use the above matrix to study the local stability of the equlibria for the model (2) as follows.

Theorem 1. *For the model (2),*

a. $E_1(0, \frac{\gamma}{\eta}, \frac{\gamma}{\eta q})$ *is locally asymptotically stable if* $\frac{r_1\eta}{\eta+k\gamma} < \alpha(1-\mu)$, *and unstable for* $\frac{r_1\eta}{\eta+k\gamma} > \alpha(1-\mu)$.

b. $E_2(\frac{\gamma}{\delta}, 0, \frac{\gamma}{\delta p})$ *is always unstable.*

Proof.

a. The variational matrix at the $E_1(0, \frac{\gamma}{\eta}, \frac{\gamma}{\eta q})$ is

$$J(E_1) = \begin{bmatrix} \frac{r_1\eta}{\eta+k\gamma} - \alpha(1-\mu) & 0 & 0 \\ \beta(1-\mu) & -r_2 & r_2q \\ -\frac{\delta\gamma}{\eta q} & -\frac{\gamma}{q} & 0 \end{bmatrix}. \tag{5}$$

The eigenvalues of $J(E_1)$ are $\lambda_1 = \frac{r_1\eta}{\eta+k\gamma} - \alpha(1-\mu)$, $\lambda_{2,3} = \frac{1}{2}(-r_2 \pm \sqrt{r_2^2 - 4r_2^2\gamma})$. Which implies, $\frac{r_1\eta}{\eta+k\gamma} > \alpha(1-\mu)$, thus E_1 is unstable, and if $\frac{r_1\eta}{\eta+k\gamma} < \alpha(1-\mu)$ then E_1 is locally asymptotically stable.

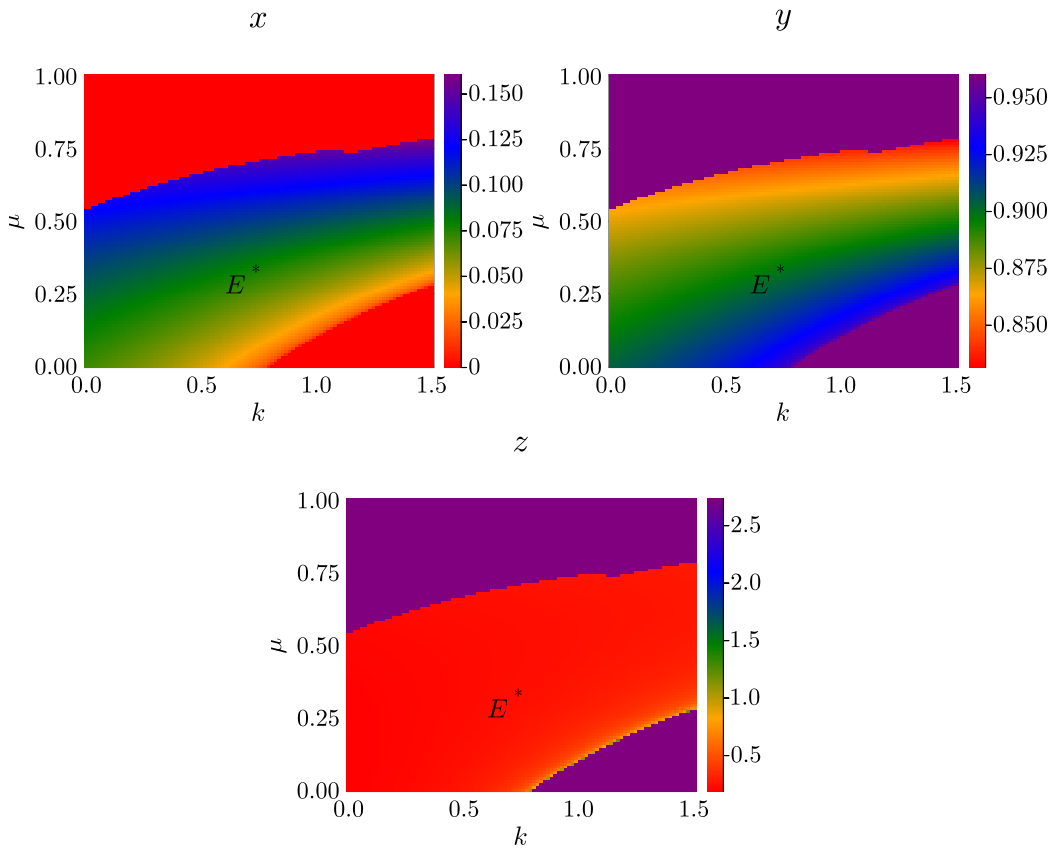

Fig. 2 The sizes of x, y, z with fix parameter values $r_1 = 1.01$, $r_2 = 0.0031$, $\gamma = 2.41$, $\delta = 2.01$, $\eta = 2.51$, $p = 0.765$, $q = 0.351$, $\beta = 0.568$, $\alpha = 0.58$, $n = 1.71$, $\mu \in (0,1)$ and $k \in (0,1.5)$.

b. The variational matrix at $E_2(\frac{\gamma}{\delta}, 0, \frac{\gamma}{\delta p})$ is

$$J(E_2) = \begin{bmatrix} -r_1 & \frac{r_1 k\gamma}{\delta n} - \frac{r_1 k\gamma}{\delta} - \alpha & r_1 p \\ 0 & r_2 + \frac{\beta}{n} & 0 \\ -\frac{\gamma}{p} & -\frac{\eta\gamma}{\delta p} & 0 \end{bmatrix}. \tag{6}$$

The eigenvalues of $J(E_2)$ are $\lambda_1 = r_2 + \frac{\beta}{n}$, $\lambda_{2,3} = \frac{1}{2}(-r_1 + r_1\gamma \pm \sqrt{(r_1\gamma - r_1)^2 - 4(r_1\gamma r_2 - \frac{r_1\gamma\beta}{n})})$. Here $\lambda_1 > 0$. So, E_2 is unstable.

■

Theorem 2. *For the model (2), the interior equilibrium $E^*(x^*, y^*, z^*)$ is locally asymptotically stable, if it satisfies $\zeta_1 > 0$, $\zeta_3 > 0$, and $\zeta_1\zeta_2 > \zeta_3$.*

Proof. The variational matrix at $E^*(x^*, y^*, z^*)$ is

$$J(E^*) = \begin{bmatrix} \hat{b}_{11} & \hat{b}_{12} & \hat{b}_{13} \\ \hat{b}_{21} & \hat{b}_{22} & \hat{b}_{23} \\ \hat{b}_{31} & \hat{b}_{32} & 0 \end{bmatrix}. \tag{7}$$

Then the characteristic polynomial of the above matrix (7) is of the form

$$\lambda^3+\zeta_1\lambda^2+\zeta_2\lambda+\zeta_3=0. \tag{8}$$

Where,

$$\zeta_1=-\hat{b}_{11}-\hat{b}_{22},\ \zeta_2=\hat{b}_{11}\hat{b}_{22}-\hat{b}_{12}\hat{b}_{21}-\hat{b}_{23}\hat{b}_{32}-\hat{b}_{13}\hat{b}_{31},\ \zeta_3=\hat{b}_{11}\hat{b}_{23}\hat{b}_{32}+\hat{b}_{13}\hat{b}_{22}\hat{b}_{31}-\hat{b}_{12}\hat{b}_{23}\hat{b}_{31}-\hat{b}_{13}\hat{b}_{21}\hat{b}_{32}.$$

$$\hat{b}_{11}=\frac{\alpha(1-\mu)^2nx^*y^*}{((1-\mu)nx^*+y^*)^2}-\frac{r_1x^*}{(1+ky^*)pz^*},\ \hat{b}_{12}=\frac{r_1kx^{*2}}{(1+ky^*)^2pz^*}-\frac{r_1kx^*}{(1+ky^*)^2}-\frac{\alpha(1-\mu)^2nx^{*2}}{((1-\mu)nx^*+y^*)^2},$$

$$\hat{b}_{13}=\frac{r_1x^{*2}}{(1+ky^*)pz^{*2}},\hat{b}_{21}=\frac{\beta(1-\mu)y^{*2}}{((1-\mu)nx^*+y^*)^2},\ \hat{b}_{22}=-\frac{\beta(1-\mu)x^*y^*}{((1-\mu)nx^*+y^*)^2}-\frac{r_2y^*}{qz^*},$$

$$\hat{b}_{23}=\frac{r_2y^{*2}}{qz^{*2}},\ \hat{b}_{31}=-\delta z^*,\ \hat{b}_{32}=-\eta z^*.$$

The coexisting equilibrium point $E^*(x^*,y^*,z^*)$ is locally asymptotically stable if $\zeta_1>0,\zeta_3>0$ and $\zeta_1\zeta_2-\zeta_3>0$ holds, that is Routh-Hurwitz criterion conditions are satisfied.

Here, $\zeta_1>0$ and $\zeta_3>0$ if

$$\frac{\alpha(1-\mu)^2nx^*y^*}{((1-\mu)nx^*+y^*)^2}-\frac{r_1x^*}{(1+ky^*)pz^*}-\frac{\beta(1-\mu)x^*y^*}{((1-\mu)nx^*+y^*)^2}-\frac{r_2y^*}{qz^*}<0,$$

$$\frac{r_1r_2\eta x^*y^{*2}}{(1+ky^*)pqz^{*2}}+\frac{r_1\delta x^{*2}}{(1+ky^*)pz^*}(\frac{\beta(1-\mu)x^*y^*}{((1-\mu)nx^*+y^*)^2}+\frac{r_2y^*}{qz^*})$$

$$+\frac{\delta r_1r_2x^{*2}y^{*2}}{(1+ky^*)^2pqz^{*2}}+(\frac{\eta r_2x^{*2}}{(1+ky^*)pz^*})(\frac{\beta(1-\mu)y^{*2}}{((1-\mu)nx^*+y^*)^2})$$

$$-\frac{r_2\alpha(1-\mu)^2n\eta x^*y^{*3}}{((1-\mu)nx^*+y^*)^2qz^*}-\frac{r_1r_2k\delta x^*y^{*2}}{(1+ky)^2qz^*}-\frac{\alpha(1-\mu)^2nr_2x^{*2}y^{*2}}{((1-\mu)nx^*+y^*)^2qz^*}>0,$$

and $\zeta_1\zeta_2-\zeta_3>0$ if

$$\frac{\alpha(1-\mu)^2ny^*}{((1-\mu)nx^*+y^*)^2}<\frac{r_1}{(1+ky^*)pz^*},\ \text{and}\ \frac{r_1kx^*}{(1+ky^*)^2pz^*}<\frac{r_1k}{(1+ky^*)^2}+\frac{\alpha(1-\mu)^2nx^*}{((1-\mu)nx^*+y^*)^2}.$$

■

Remark 1. The model (2) is not well-defined at the origin $(0,0,0)$ and thus cannot be linearized at $(0,0,0)$. This is the main reason for model (2) to have very rich and complicated dynamics. In [30,31], the authors considered the two-dimensional ratio-dependent predator prey model and redefining the system at $(0,0)$ and making a transformation in the time variable, transform to new system and studied the behavior of the trajectories near $(0,0)$. They showed that solution orbit of new system tends to the origin then it must tend to it along a fixed direction. We show the trajectories near the origin for the model (2) in the numerical section.

2.3 Hopf-bifurcation analysis

In order to investigate the bifurcation behavior of the model (2), we analyze the dynamical changes associated with the prey refuge parameter and obtain the critical value of the prey refuge μ. The below theorem shows the presence of Hopf-bifurcation, along with the prey refuge parameter, as a bifurcation parameter.

Theorem 3. *The model (2) experiences Hopf-bifurcation near the coexisting equilibrium point $E^*(x^*,y^*,z^*)$ if the bifurcation parameter μ passes the critical value. The necessary and sufficient condition for the occurrence of Hopf-bifurcation at $\mu=\mu^*$ are*

a. $\zeta_1(\mu^*)\zeta_2(\mu^*) - \zeta_3(\mu^*) = 0$.

b. $\frac{d}{d\mu^*}(Re(\lambda(\mu^*)))|_{\mu=\mu^*} \neq 0$.

Where, λ is the zero of the characteristic polynomial associated with an coexisting equilibrium point E^*.

Proof. For $\mu = \mu^*$, let the characteristic Eq. (8) be in the from

$$(\lambda^2(\mu^*) + \zeta_2(\mu^*))(\lambda(\mu^*) + \zeta_1(\mu^*)) = 0. \tag{9}$$

Which gives that, $\pm i\sqrt{\zeta_2(\mu^*)}$ and $-\zeta_1(\mu^*)$ be the roots of (9). To obtain the Hopf-bifurcation at $\mu = \mu^*$, it necessary to fulfill the transversality condition $\frac{d}{d\mu^*}(Re(\lambda(\mu^*)))|_{\mu=\mu^*} \neq 0$. For all μ, the general roots of the above Eq. (9) are given by $\lambda_{1,2} = u(\mu) \pm iv(\mu)$, $\lambda_3 = -\zeta_2(\mu)$.

Next, substituting $\lambda_{1,2}(\mu) = u(\mu) + iv(\mu)$ into (9) we get

$$F_1(\mu) + iF_2(\mu) = 0,$$

where,

$$\begin{aligned} F_1(\mu) =& u^3(\mu) + u^2(\mu)\zeta_1(\mu) - 3u(\mu)v^2(\mu) - v^2(\mu)\zeta_1(\mu) + \zeta_2(\mu)u(\mu) + \zeta_1(\mu)\zeta_2(\mu), \\ F_2(\mu) =& \zeta_2(\mu)v(\mu) + 2u(\mu)v(\mu)\zeta_1(\mu) + 3u^2(\mu)v(\mu) - v^3(\mu). \end{aligned}$$

In order to fulfill the (9) we must have $F_1(\mu) = 0$ and $F_2(\mu) = 0$, then differentiate $F_1(\mu)$ and $F_2(\mu)$ with respect to μ, we have

$$\frac{dF_1}{dm} = \Phi_1 u'(\mu) - \Phi_2 v'(\mu) + \Phi_3 = 0, \tag{10}$$

$$\frac{dF_2}{dm} = \Phi_2(\mu)u'(\mu) + \Phi_1(\mu)v'(\mu) + \Phi_4 = 0. \tag{11}$$

Where,

$$\begin{aligned} \Phi_1(\mu) &= 3u^2(\mu) + 2u(\mu)\zeta_1(\mu) - 3v'(\mu) + \zeta_2(\mu), \\ \Phi_2(\mu) &= 6v(\mu)u(\mu) + 2v(\mu)\zeta_1(\mu), \\ \Phi_3(\mu) &= u^2(\mu)\zeta_1'(\mu) + \zeta_2'(\mu)u(\mu), \\ \Phi_4(\mu) &= 2u(\mu)v(\mu)\zeta_1'(\mu) + \zeta_2'(\mu)v(\mu). \end{aligned}$$

On multiply (10) and (11) by $\Phi_1(\mu)$ and $\Phi_2(\mu)$ respectively, then on simplification we have

$$u'(\mu) = -\frac{\Phi_1(\mu)\Phi_3(\mu) + \Phi_2(\mu)\Phi_4(\mu)}{\Phi_1^2(\mu) + \Phi_2^2(\mu)}. \tag{12}$$

Substituting $u(\mu) = 0$ and $v(\mu) = \sqrt{\zeta_2(\mu)}$ at $\mu = \mu^*$ on $\Phi_1(\mu), \Phi_2(\mu)$, $\Phi_3(\mu)$ and $\Phi_4(\mu)$, then substituting into above Eq. (12), we get

$$u'(\mu) = \frac{\zeta_3'(\mu^*) - (\zeta_1(\mu^*)\zeta_2(\mu^*))'}{2(\zeta_2^2(\mu^*) + \zeta_1^2(\mu^*))}.$$

If $\zeta_3'(\mu^*) - (\zeta_1(\mu^*)\zeta_2(\mu^*))' \neq 0$, which implies that

$$\frac{d}{d\mu^*}(Re(\lambda_j(\mu^*)))|_{\mu=\mu^*} \neq 0, \quad j = 1, 2,$$

and $\lambda_3(\mu^*) = -\zeta_2(\mu^*)$.

Therefore, the condition $\zeta_3'(\mu^*) - (\zeta_1(\mu^*)\zeta_2(\mu^*))' \neq 0$ is guaranteed that the above transversality condition holds, thus the model (2) has enter into Hopf-bifurcation at $\mu = \mu^*$. ■

3 Model with time delay

This section's goal is to examine model (2) by including the gestation delay as an additional factor. A very significant part of each and every one of the interactions that make up ecology is played by a set of differential equations that include time delays. Since a delay in time may cause a stable equilibrium to become unstable and the population to oscillate, delay differential equations, in general, show significantly more complex dynamics than ordinary differential equations do. This is due to the fact that a time delay can cause a population to oscillate. The authors of [32] investigated the dynamics of the food chain model by taking into account the implications of middle predator gestation delay and the Allee effect on the population of prey. They discovered that the Allee effect and gestation delay both help to sustain the proposed model. The intraguild predation model with a ratio-dependent functional response was described by the authors in [11] in relation to the effects of gestational delay. It is generally accepted to make the assumption that the transformation of prey biomass into predator biomass does not occur instantly, and that there is also a lag time involved in the gestation process. Then model (2) takes the following form

$$\begin{aligned}
\frac{dx}{dt} &= \frac{r_1 x}{1+ky}(1-\frac{x}{pz}) - \frac{\alpha(1-\mu)xy}{(1-\mu)nx+y)},\\
\frac{dy}{dt} &= r_2 y(1-\frac{y}{qz}) + \frac{\beta(1-\mu)x(t-\tau)y(t-\tau)}{(1-\mu)nx(t-\tau)+y(t-\tau)},\\
\frac{dz}{dt} &= z(\gamma-\delta x-\eta y).
\end{aligned} \tag{13}$$

Subjected to the initial conditions $x(l)=\psi_1(l)\geq 0$, $y(l)=\psi_2(l)\geq 0$ and $z(l)=\psi_3(l)\geq 0$, where $l\in[-\tau,0]$, $\psi_i(l)\in C([-\tau,0]\to R^+),(i=1,2,3)$ and τ represents the gestation time lag.

3.1 Local stability and Hopf-bifurcation analysis

The above model (13) can be given by

$$\frac{dW(t)}{dt} = G(W(t),W(t-\tau)),$$

where $W(t)=[x(t),y(t),z(t)]^T, W(t-\tau)=[x(t-\tau),y(t-\tau),z(t-\tau)]^T$.

Let $x(t)=x^*+\bar{p}(t), y(t)=y^*+\bar{q}(t)$ and $z(t)=z^*+\bar{s}(t)$. Then linearized model (13) near the coexisting equilibrium point $E^*(x^*,y^*,z^*)$, we find

$$\frac{d\chi}{dt} = R\chi(t)+S\chi(t),$$

where $R=(\frac{\partial G}{\partial W(t)})$, $S=(\frac{\partial G}{\partial W(t-\tau)})$ and $\chi=[\bar{p}(t),\bar{q}(t),\bar{s}(t)]^T$.

Thus, the variational matrix of the model (13) at $E^*(x^*,y^*,z^*)$ is of the form

$$J(E^*) = R+Se^{-\lambda\tau} = \begin{bmatrix} \hat{c}_1 & \hat{c}_2 & \hat{c}_3 \\ \hat{c}_4 e^{-\lambda\tau} & \hat{c}_5+\hat{c}_6 e^{-\lambda\tau} & \hat{c}_7 \\ \hat{c}_8 & \hat{c}_9 & \hat{c}_{10} \end{bmatrix}, \tag{14}$$

where

$$\hat{c}_1 = \frac{r_1}{1+ky^*} - \frac{2r_1x^*}{(1+ky^*)pz^*} - \frac{\alpha(1-\mu)y^{*2}}{(n(1-\mu)x^*+y^*)^2}, \hat{c}_2 = \frac{r_1kx^{*2}}{(1+ky^*)^2pz^*} - \frac{r_1kx^*}{(1+ky^*)^2} - \frac{\alpha(1-\mu)^2nx^{*2}}{((1-\mu)nx^*+y^*)^2},$$
$$\hat{c}_3 = \frac{r_1x^{*2}}{(1+ky)pz^{*2}}, \hat{c}_4 = \frac{\beta(1-\mu)y^{*2}}{((1-\mu)nx+y)^2}, \hat{c}_5 = r_2 - \frac{2r_2y^*}{qz^*}, \hat{c}_6 = \frac{\beta(1-\mu)x^{*2}n}{((1-\mu)nx+y)^2}, \hat{c}_7 = \frac{r_2y^{*2}}{qz^{*2}},$$

$\hat{c}_8 = -\delta z^*,\ \hat{c}_9 = -\eta z^*,\ \hat{c}_{10} = \gamma - \delta x^* - \eta y^*.$

The characteristic polynomial of above variational matrix (14) is given by

$$\lambda^3 + (\rho_1\lambda^2 + \rho_2\lambda + \rho_3) + (\rho_4\lambda^2 + \rho_5\lambda + \rho_6)e^{-\lambda\tau} = 0. \tag{15}$$

Where

$$\begin{aligned}
\rho_1 &= -\hat{c}_1 - \hat{c}_5 - \hat{c}_{10},\ \rho_2 = \hat{c}_1\hat{c}_5 + \hat{c}_1\hat{c}_{10} + \hat{c}_5\hat{c}_{10} - \hat{c}_7\hat{c}_9 - \hat{c}_3\hat{c}_8,\\
\rho_3 &= -\hat{c}_1\hat{c}_5\hat{c}_{10} + \hat{c}_1\hat{c}_7\hat{c}_9 - \hat{c}_2\hat{c}_7\hat{c}_8 + \hat{c}_8\hat{c}_5\hat{c}_3, \rho_4 = -\hat{c}_6,\\
\rho_5 &= \hat{c}_1\hat{c}_6 - \hat{c}_6\hat{c}_{10} - \hat{c}_2\hat{c}_4, \rho_6 = \hat{c}_1\hat{c}_6\hat{c}_{10} + \hat{c}_1\hat{c}_4\hat{c}_{10} - \hat{c}_3\hat{c}_4\hat{c}_9 + \hat{c}_3\hat{c}_8\hat{c}_9.
\end{aligned}$$

Case-I When $\tau = 0$, then the above Eq. (15) becomes

$$\lambda^3 + (\rho_1 + \rho_4)\lambda^2 + (\rho_2 + \rho_5)\lambda + (\rho_3 + \rho_6) = 0. \tag{16}$$

The characteristic polynomial (16) is similar to the characteristic polynomial (8) of the model (2) in previous Section 2. By the Routh-Hurwitz criterion, all the zeros of (16) have negative real parts if and only if $(\rho_1 + \rho_4) > 0,\ (\rho_1 + \rho_4)(\rho_2 + \rho_5) > (\rho_3 + \rho_6)$.

Case-II When $\tau > 0$, let $\lambda = iu$ $(u > 0)$ be a zero of (15), then we have

$$-iu^3 - u^2\rho_1 + iu\rho_2 + \rho_3 + (-\rho_4 u + iu\rho_5 + \rho_6)(\cos u\tau - i\sin u\tau) = 0.$$

Separating real and imaginary parts, we get

$$\rho_1 u^2 - \rho_3 = (\rho_6 - u^2\rho_4)\cos u\tau + u\rho_5 \sin u\tau, \tag{17}$$

$$u\rho_2 - u^3 = -u\rho_5 \cos u\tau + (\rho_6 - u^2\rho_4)\sin u\tau. \tag{18}$$

Adding up the squares of both equations, we obtain

$$u^6 + (\rho_1^2 - 2\rho_2 - \rho_4^2)u^4 + (\rho_2^2 - 2\rho_1\rho_3 + 2\rho_4\rho_6 - \rho_5^2)u^2 + (\rho_3^2 - \rho_6^2) = 0. \tag{19}$$

Denote $u^2 = h$, then (19) becomes

$$h^3 + L_1h^2 + L_2h + L_3 = 0, \tag{20}$$

where $L_1 = \rho_1^2 - 2\rho_2 - \rho_4^2$, $L_2 = \rho_2^2 - 2\rho_1\rho_3 + 2\rho_4\rho_6 - \rho_5^2$, $L_3 = \rho_3^2 - \rho_6^2$. Let

$$g(h) = h^3 + L_1h^2 + L_2h + L_3 = 0 \tag{21}$$

Let us use the roots of (21) to study the distribution of roots of (15).

Lemma 4. *Equation (20) has at least one positive real zero.*

Proof. Clearly $\lim_{h\to+\infty} g(h) = +\infty$ and $g(0) = L_3 < 0$, if $\rho_3^2 < \rho_6^2$. From (21) we can assures that is have one positive zero if $\rho_3^2 < \rho_6^2$.

Hence, there exist a $h_0 \in (0, +\infty)$ such that $g(h_0) = 0$. Assume, h_1, h_2, and h_3 are the zeros of Eq. (21). Then $\hat{u}_i = \sqrt{h_i},\ i = 1, 2, 3$.

From (17) and (18) we have

$$\sin u_i\tau = \frac{(u_i{}^2\rho_1 - \rho_3)\rho_5 u_i - (u_i{}^3 - u_i\rho_2)(\rho_6 - \rho_4 u_i{}^2)}{(u_i\rho_5)^2 + (\rho_6 - \rho_4 u_i{}^2)^2},$$

$$\tau_i^{(j)} = \frac{1}{u_i}\{\arcsin[\frac{(u_i{}^2\rho_1\rho_3)\rho_5 u_i - (u_i{}^3 - u_i\rho_2)(\rho_6 - \rho_4 u_i{}^2)}{(u_i\rho_5)^2 + (\rho_6 - \rho_4 u_i{}^2)^2}] + 2j\pi\},$$

for $i = 1,2,3,\ j = 0,1,2,\ldots$. Then, $\pm iu_i$ are a pair of purely imaginary zeros of (15) with $\tau = \tau_i^{(j)}$. Define $\hat{\tau} = \tau_i^{(0)} = \min_{i\in 1,2,3}\{\tau_i^{(0)}\}, \hat{u} = u_{i_0}$. Now, we take $\lambda(\tau) = v + iu$ be the zero of (15) near $\tau = \hat{\tau}$ fulfilling $v(\hat{\tau}) = 0, u(\hat{\tau}) = \hat{u}$. ■

Then we have the following lemma.

Lemma 5. *If $2u^6 + (\rho_1^2 - 2\rho_2 - \rho_4^2) - \rho_5^2 + \rho_6^2 \neq 0$, holds the transversality condition is satisfied:*

$$Re\{(\frac{d\lambda(\tau)}{d\tau})^{-1}\}_{\tau=\hat{\tau}} \neq 0.$$

Proof. From (15) we have

$$\frac{d}{d\tau}[\lambda^3 + (\rho_1\lambda^2 + \rho_2\lambda + \rho) + (\rho_4\lambda^2 + \rho\lambda + \rho_6)e^{-\lambda\tau}] = 0,$$

$$[3\lambda^2 + 3\rho_1\lambda + \rho_2 + (2\rho_4\lambda + \rho - \tau(\rho_4\lambda^2 + \rho_5\lambda + \rho_6)e^{-\lambda\tau})]\frac{d\lambda}{d\tau} = \lambda(\rho_4\lambda^2 + \rho_5\lambda + \rho)e^{-\lambda\tau},$$

$$(\frac{d\lambda}{d\tau})^{-1} = \frac{3\lambda^2 + 2\rho_1\lambda + \rho_2}{\lambda(\rho_4\lambda^2 + \rho_5\lambda + \rho_6)e^{-\lambda\tau}} + \frac{2\rho_4\lambda + \rho_5}{\lambda(\rho_4\lambda^2 + \rho_5\lambda + \rho_6)} - \frac{\tau}{\lambda},$$

$$Re\{(\frac{d\lambda}{d\tau})^{-1}\}_{\lambda=iu} = \frac{2u^6 + (\rho_1^2 - 2\rho_2 - \rho_4^2) - \rho_5^2 + \rho_6^2}{u^2(\rho_6 - \rho_4 u^2)^2 + u^2(\rho_5 u)^2} \neq 0,$$

if $2u^6 + (\rho_1^2 - 2\rho_2 - \rho_4^2) - \rho_5^2 + \rho_6^2 > 0$. ■

The existence of Hopf-bifurcation at $\tau = \hat{\tau}$ is ensured by Lemma 4 and 5, the switching behavior of model (13) around $E^*(x^*, y^*, z^*)$ is stated below.

Theorem 6. *Assume that E^* of the model (13) exists and it is locally asymptotically stable at $\tau = 0$. Also, let $v = u^2$ be the positive root of (16).*

1. *Then there exists $\tau = \hat{\tau}$ such that E^* is locally asymptotically stable for $0 \leq \tau < \hat{\tau}$ and unstable for $\tau > \hat{\tau}$.*
2. *Also, the model (13) can exhibits the Hopf-bifurcation at E^* when $\tau = \hat{\tau}$ provided $2u^6 + (\rho_1^2 - 2\rho_2 - \rho_4^2) - \rho_5^2 + \rho_6^2 \neq 0$.*

3.2 Direction and stability of Hopf bifurcation

The quantities of bifurcation periodic solutions in the center manifold as $\hat{\tau}$, using the results from [33,34], we have the following theorem:

Theorem 7. *For model (13), the following results hold:*

(i) The sign of μ_2 determines the Hopf bifurcation: if $\mu_2 > 0$ ($\mu < 0$), then the Hopf bifurcation is supercritical (subcritical) and the bifurcation periodic solution exist for $\tau > \hat{\tau}$ ($\tau < \hat{\tau}$).

(ii) The sign of β_2 determines the stability of the bifurcating periodic solution: the bifurcation periodic solution are stable (unstable) if $\beta < 0$ ($\beta > 0$).

(iii) The sign of T_2 determines the period of the bifurcating periodic solutions: the periodic increase (decrease) if $T_2 > 0$ ($T_2 < 0$).

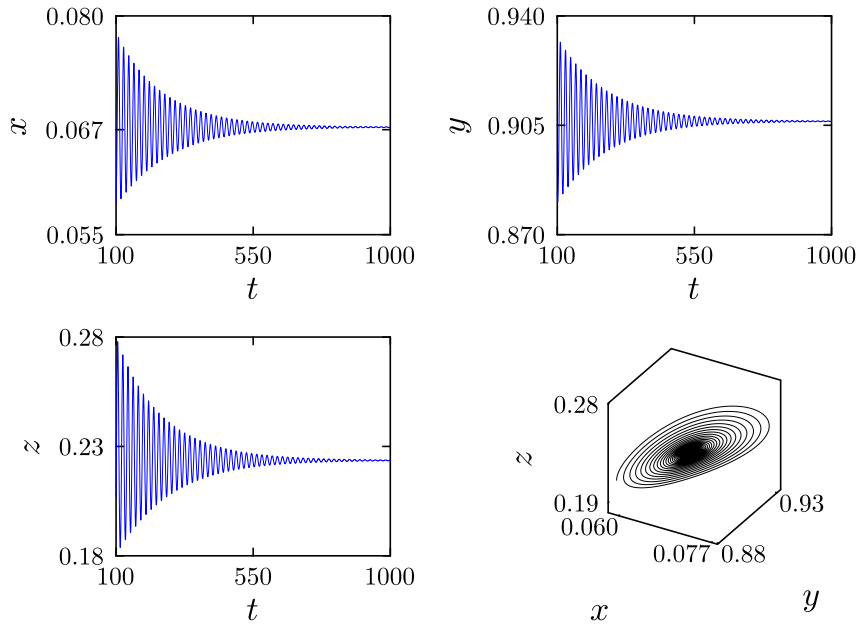

Fig. 3 The time evaluation of intraguild prey, intraguild predator and biotic resource, and the phase trajectory for the model (2) with $\mu = 0.14$ and $k = 0.4$.

Proof. See Appendix A. ■

Remark 2. We omit the stability of the Hopf bifurcation in the non-delay cases due to the length of the paper. Nevertheless, they are straightforward and calculable.

Remark 3. In Section 2, the condition for local stability and the existence of Hopf bifurcation near the interior equilibrium point are discussed. Theorem 1 is necessary to state that the equilibrium E^* is locally asymptotically stable for the non-delayed model (2). Similarly, for the delayed model (13), the local stability results are stated in Theorem 6. In the absence of delay $\tau = 0$, the model (13) is reduced to the model (2), and the stability property is given by the Theorem 2.

Remark 4. To begin, we extended the ratio-dependent type of intraguild predation model investigated in [5, 11] by considering the fear effect in the prey population. The consideration of the fear effect in other types of predator-prey models has been extensively studied by many researchers [16, 20, 35, 36]. Furthermore, applied mathematics and theoretical ecology both acknowledge the importance of studying the effects of prey refuge on the dynamics of prey-predator interactions [17, 21, 37]. Moreover, the delay in the predator-prey model has been explored by many researchers [22–24, 32] due to its need. Since further research is required to improve our understanding of the biological relationship, we made an effort to investigate the significance of taking the fear effect into account while analyzing the dynamical changes induced by the fear effect in the intraguild predation model with prey refuge.

4 Numerical simulation

To validate the analytical results obtained in the preceding sections, we conduct the numerical simulations for the systems (2) and (13) in this section:

We just take into account a small range of possible parameter values [3, 4, 29], such as

$$\begin{aligned} r_1 = 1.01, r_2 = 0.0031, \gamma = 2.41, \delta = 2.01, \eta = 2.51, \\ p = 0.765, q = 0.351, \beta = 0.568, \alpha = 0.58, \text{ and } n = 1.71. \end{aligned} \tag{22}$$

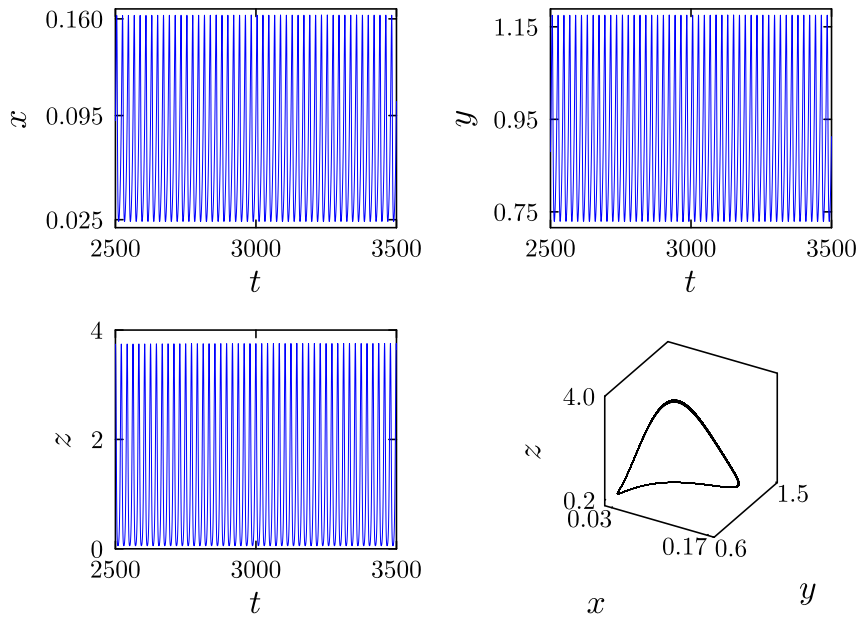

Fig. 4 The time evaluation of intraguild prey, intraguild predator and biotic resource, and the phase trajectory for the model (2) at $\mu = 0.14$ and $k = 0.7$.

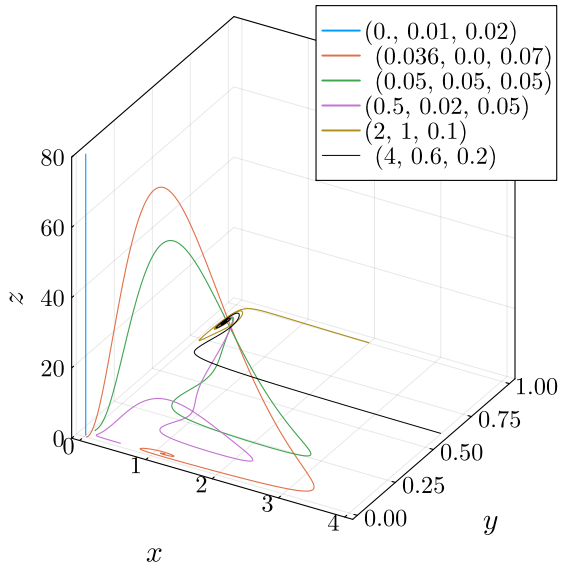

Fig. 5 The time evaluation of intraguild prey, intraguild predator and biotic resource; (d) the phase trajectory for the model (2) at $\mu = 0.14$ and $k = 0.7$.

The model (2) has three equilibrium points for the given set of parameter values, namely E_1, E_2 and E^*, respectively. The based on eigenvalues of the variational matrix (5) of the model (2) at E_1 is unstable if $\frac{r_1\eta}{\eta+k\gamma} > \alpha(1-\mu)$, and if $\frac{r_1\eta}{\eta+k\gamma} < \alpha(1-\mu)$ then E_1 is locally asymptotically stable, and eigenvalues of the variational matrix (6) for the model (2) at E_2 is unstable. For various value of k, the existence of different equilibrium points and its stability nature is given in Table 1.

First, for small amount of fear effect $k = 0.4$, the model (2) has $E_1(0, 0.960159, 2.7355)$ and its

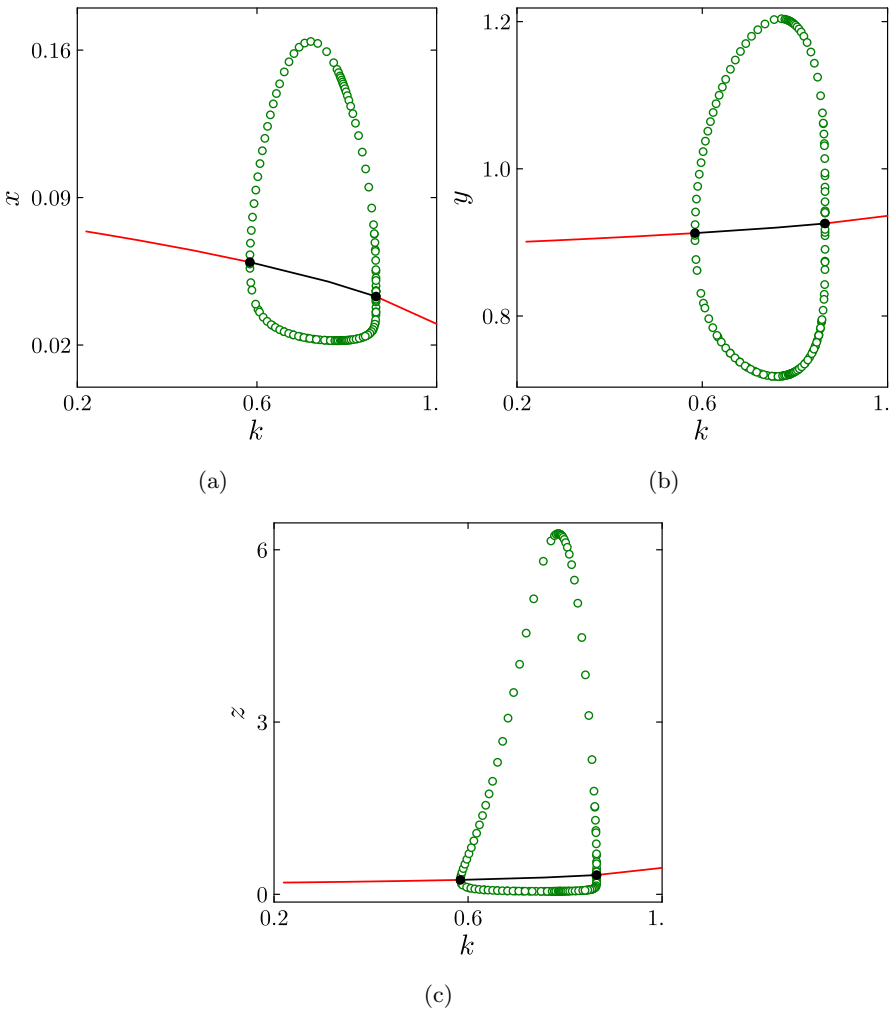

Fig. 6 (a) k vs $x(t)$, (b) k vs $y(t)$, & (c) k vs $z(t)$; The bifurcation diagrams for the model with $k \in (0.2, 1)$ and $\mu = 0.14$. The red solid lines represent the stable equilibrium points, while the black solid lines represent the unstable equilibrium points. The green circles represents the maximum and minimum values of the stable periodic solutions, and the black points represent the Hopf bifurcation points.

Table 1 Equilibrium points and its stability for various values of k.

k value	Equilibria	Eigenvalues	Stability
0.2	(0.0712264,0.903121, 0.204243)	$\lambda_1 = -0.38209$, $\lambda_{2,3} = -0.01431 \pm 0.401581i$	Asymptotically stable
0.493	(0.0591405,0.9128, 0.242695)	$\lambda_1 = -0.23943$, $\lambda_{2,3} = \pm 0.344281i$	Periodic orbit
0.95	(0.0236362,0.941232, 0.537717)	$\lambda_1 = -0.0280049$, $\lambda_{2,3} = -0.005647 \pm 0.202492i$	Asymptotically stable

corresponding eigenvalues are $\lambda_1 = 0.230935$, $\lambda_{2,3} = -0.00155 \pm 0.086421i$, hence E_1 is unstable. Also, $E_2(1.199, 0, 1.56733)$ exists and its corresponding eigenvalues are $\lambda_1 = 0.335264$, $\lambda_{2,3} = -0.505 \pm 1.47617i$, which is unstable. Similarly, there exists an interior equilibrium point $E^*(0.0672843, 0.906278, 0.223604)$ and it is locally asymptotically stable, see in Fig.3. For different values of k the values of interior

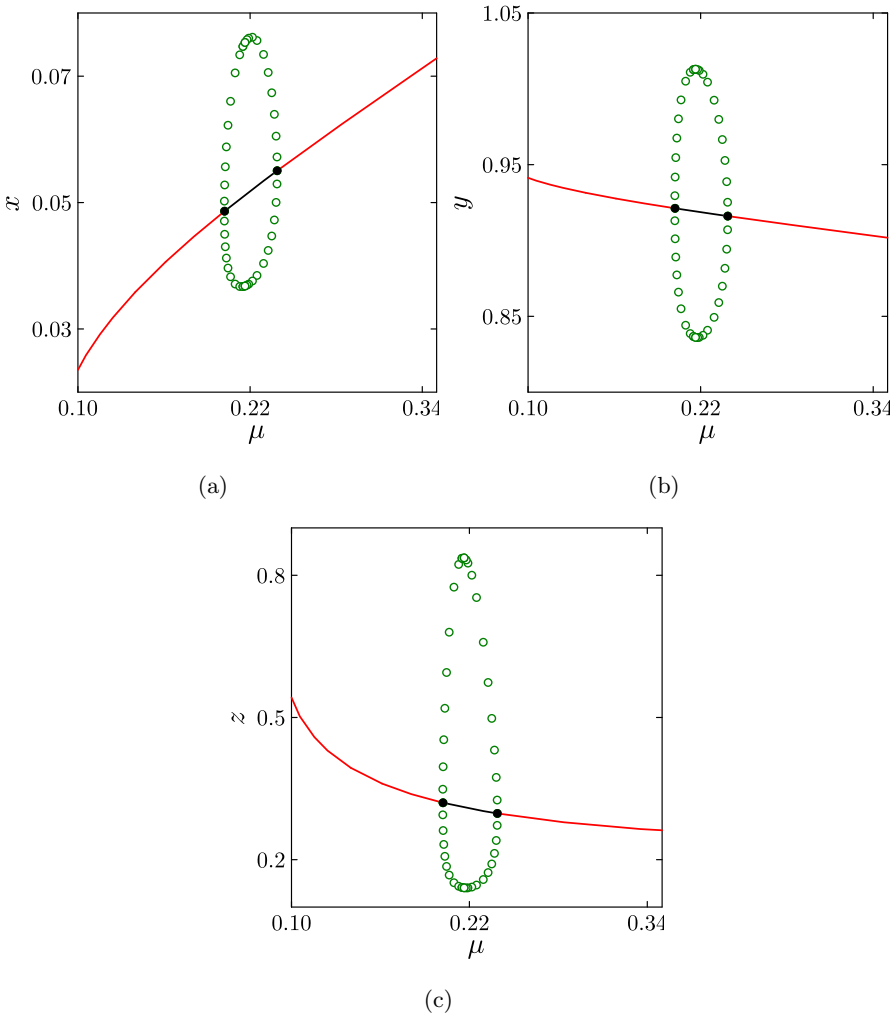

Fig. 7 (a) μ vs $x(t)$, (b) μ vs $y(t)$, & (c) μ vs $z(t)$; The bifurcation diagrams for the model (2) with $\mu \in (0.1, 0.34)$, and $k = 0.95$. The red solid lines represent the stable equilibrium points, while the black solid lines represent the unstable equilibrium points. The green circles represents the maximum and minimum values of the stable periodic solutions, and the black points represent the Hopf bifurcation points.

equilibrium and its corresponding eigenvalues with stability nature is given in Table 1. By increasing the cost of fear $k = 0.311$ then the model (2) losses its stability and oscillates near the coexisting equilibrium $E^*(0.0593516, 0.0912631, 0.251141)$, arise limit cycle, it shown in Fig.4. Furthermore, increasing the cost of fear $k > 1.5$ the prey and biotic resources will extinct. It is shown that the prey and biotic resources decreases as fear strength increases. Further, the fear in the prey population alone can cause changes in the dynamics of the proposed non-delayed model (2). To see the dynamics of the model (2), the bifurcation diagram is plotted by taking $\mu = 0.14$ and varying the fear parameter $k \in (0, 1)$ is shown in Fig.6. To show the influence of refuge parameter, the one parameter bifurcation diagram is plotted in 7 for $\mu \in (0.1, 0.5)$ with $k = 0.95$ and all other parameters are same as in (22). When $\mu = 0.21$ and $k = 0.95$ then $E^*(0.05005, 0.92008, 0.31452)$ is losses its stability and attains Hopf-bifurcation. For the clear representation, the dynamics changes of the model (2) with the consequences of fear and prey refuge are shown in Fig.6 and 7, respectively. From the derivation in the section 2.3, we have the result $\zeta_1(\mu^*)\zeta_2(\mu^*) - \zeta_3(\mu^*) = 0.00030$, and $\zeta_3'(\mu^*) - (\zeta_1(\mu^*)\zeta_2(\mu^*))' = 0.0038 \neq 0$, at $\mu = 0.14$ and $k = 0.95$. This validated the result of Theorem 3. It is clear from Fig 6 and 7, the stable periodic solution

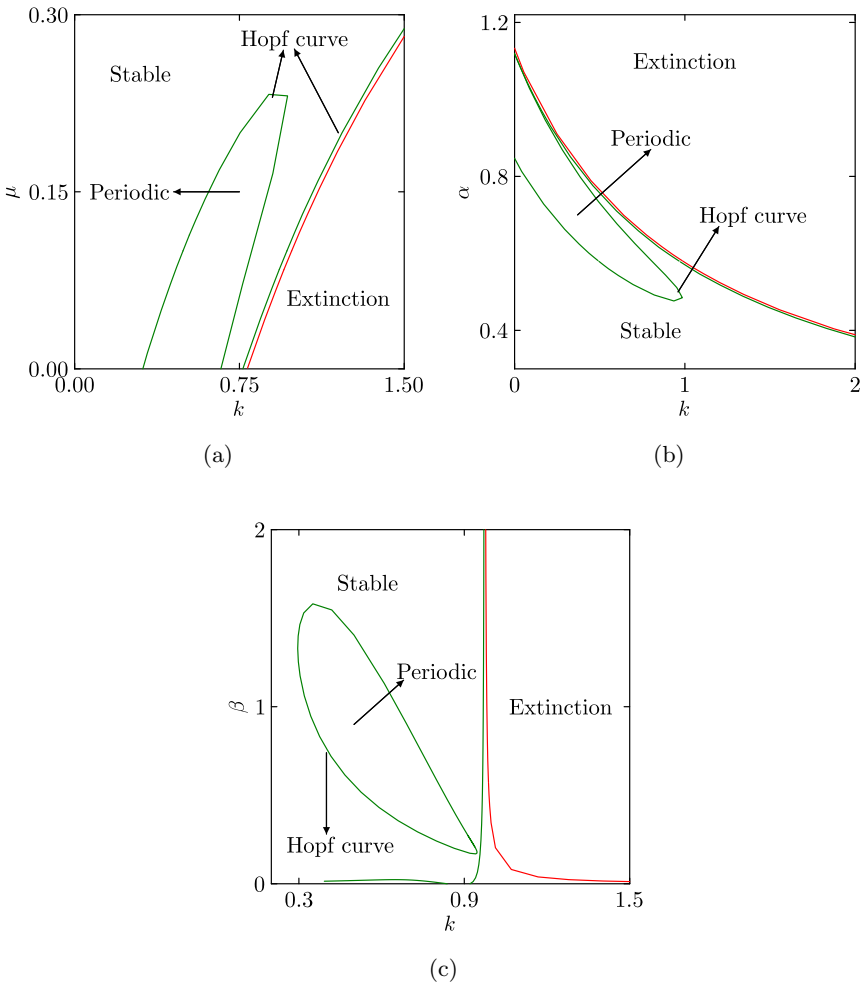

Fig. 8 (a) k vs μ, (b) k vs α, & (c) k vs β; The two parameter bifurcation diagrams for the model (2) with different values of the model parameters. The green line represents the Hopf curve which separates stable and periodic region. The red line represents the extinction boundary.

starts appear from the Hopf bifurcation points. Further, it is important to show the influence of fear parameter and prey refuge with other model parameters. We plotted the two parameter bifurcation diagram by taking k, μ, p, and q as a bifurcation parameter and showed the stable, periodic, and extinction region in Fig.8. The extinction region tells either of the species become extinct if it cross the parametric boundary. This one and two parameter bifurcation diagram is plotted using XPPAUT AUTO bifurcation tool [38, 39].

Next, we show the dynamical changes of the delayed model (13) by taking τ as a bifurcation parameter. Fix the values of prey refuge and fear effect are $\mu = 0.14$ and $k = 0.5$, respectively, and varying time delay in the range $\tau \in (0, 1]$. We have the coexisting equilibrium point $E^*(0.0631537, 0.909586, 0.237158)$. The coexisting equilibrium point E^* is locally asymptotically stable for $\tau \in (0, 0.191098)$, losses its stability and undergoes Hopf-bifurcation when the time delay crosses the threshold value $\hat{\tau} = 0.191098$. Also, the transversality condition $Re\{(\frac{d\lambda}{d\tau})^{-1}\}_{\lambda=iu} = 21.3879 \neq 0$ from Lemma 5. The locally asymptotically stable E^* for $\tau = 0.05$ is shown in Fig.9 and occurrence of periodic oscillations for $\tau = 0.22$ is depicted in Fig.10. To show the presence of Hopf-bifurcation, the bifurcation diagram is plotted in Fig.11 for $\mu = 0.14, k = 0.5$ and $\tau \in (0.1, 1)$. Then, we choose $\hat{\tau} = 0.2$ and from

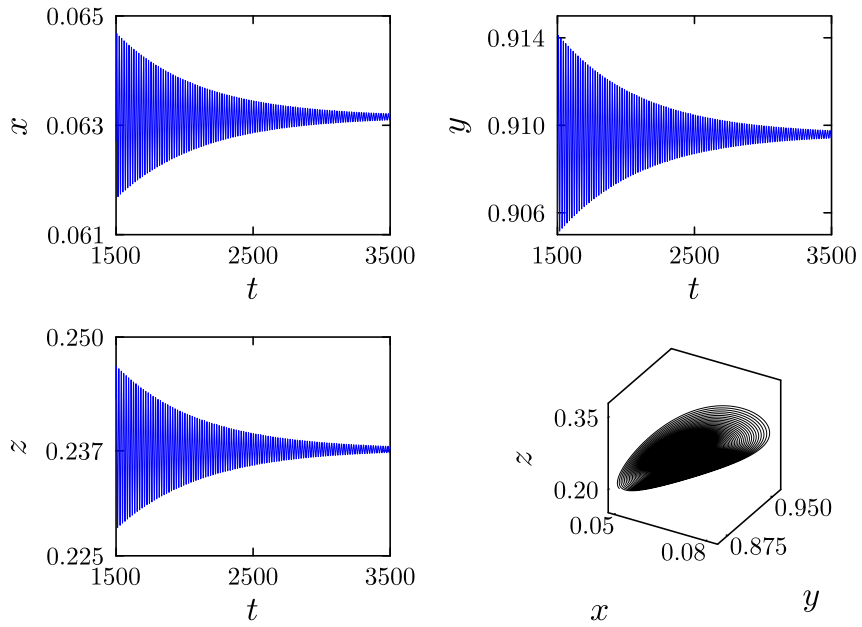

Fig. 9 The time evaluation of intraguild prey, intraguild predator and biotic resource, and the phase trajectory for the model (13) when $\tau = 0.05$, $\mu = 0.14$ and $k = 0.5$.

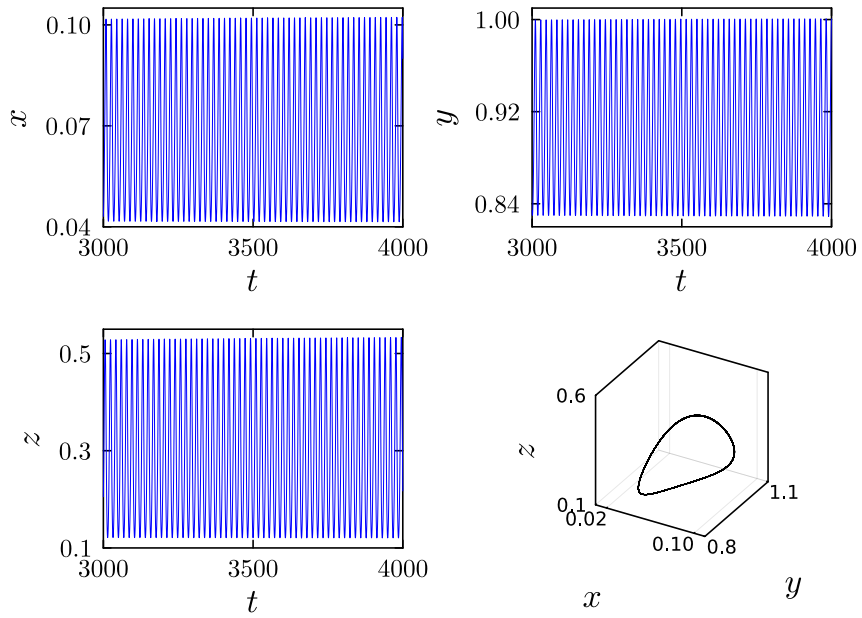

Fig. 10 The time evaluation of intraguild prey, intraguild predator and biotic resource, and the phase trajectory for the model (13) when $\tau = 0.22$, $\mu = 0.14$ and $k = 0.5$.

formulae (A9), it follows that $\hat{c_1}(0) = 2.28 - 1.115i$, $\mu_2 = -19.72 < 0$, $\beta_2 = 44.57 > 0$ and $T_2 = 16.74 > 0$. Form Theorem 7, we know the Hopf bifurcation is subcritical, the bifurcating periodic solutions exist as $\tau > \tau_0$ and the bifurcating periodic solution from E^* is unstable and increases.

Further, to show the effect of time delay in the periodic state, we choose the $k = 0.7$ and the bifurcation diagram is plotted for $\tau \in (0, 8)$ in Fig.12. It is clearly shown that the transition of periodic

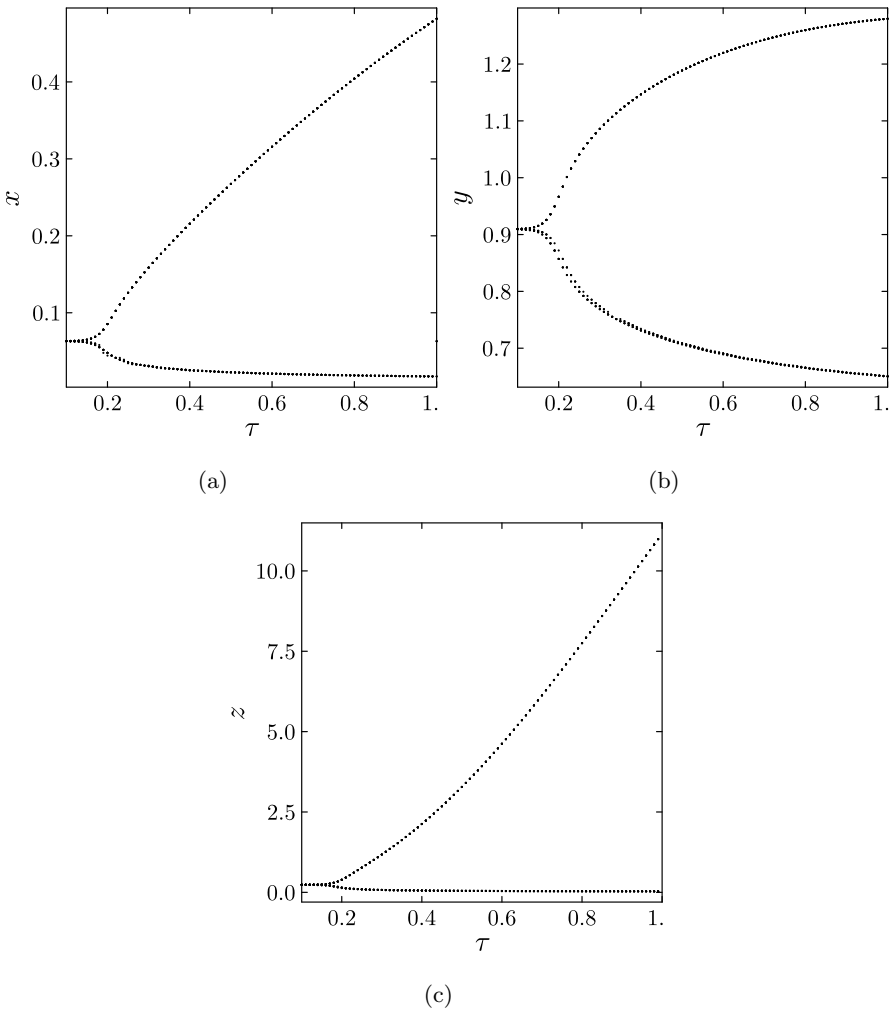

Fig. 11 (a) τ vs $x(t)$, (b) τ vs $y(t)$, & (c) τ vs $z(t)$; The bifurcation diagrams for the model (13) with $\tau \in (0,1)$, $\mu = 0.14$ and $k = 0.5$.

oscillation to stable state, when the time delay crosses the critical value $\tau = 0.701$. Finally, the influence of time delay are shown with respect to prey refuge and fear effect, the two parameter bifurcation diagram is plotted in Fig.13.

The numerical simulation ensure that the coexisting equilibrium E^* is found for the proposed model to ensure that all three species exist and interact each other. Following that, the locally asymptotically stable trajectories near E^* state that current population changes have no effect on future time. The periodic solution implies that the size of populations oscillates between two extreme points. This phenomena is also examined when time delay is taken into account.

5 Conclusion

Relatively recently, a variety of field experiments and research have demonstrated that predators influence the prey population not only by directly killing them but also by instilling fear in the prey population, which affects the reproduction rate of the prey population. This has been shown to be one of the primary ways in which predators exert their influence on the prey population. In light of this fact,

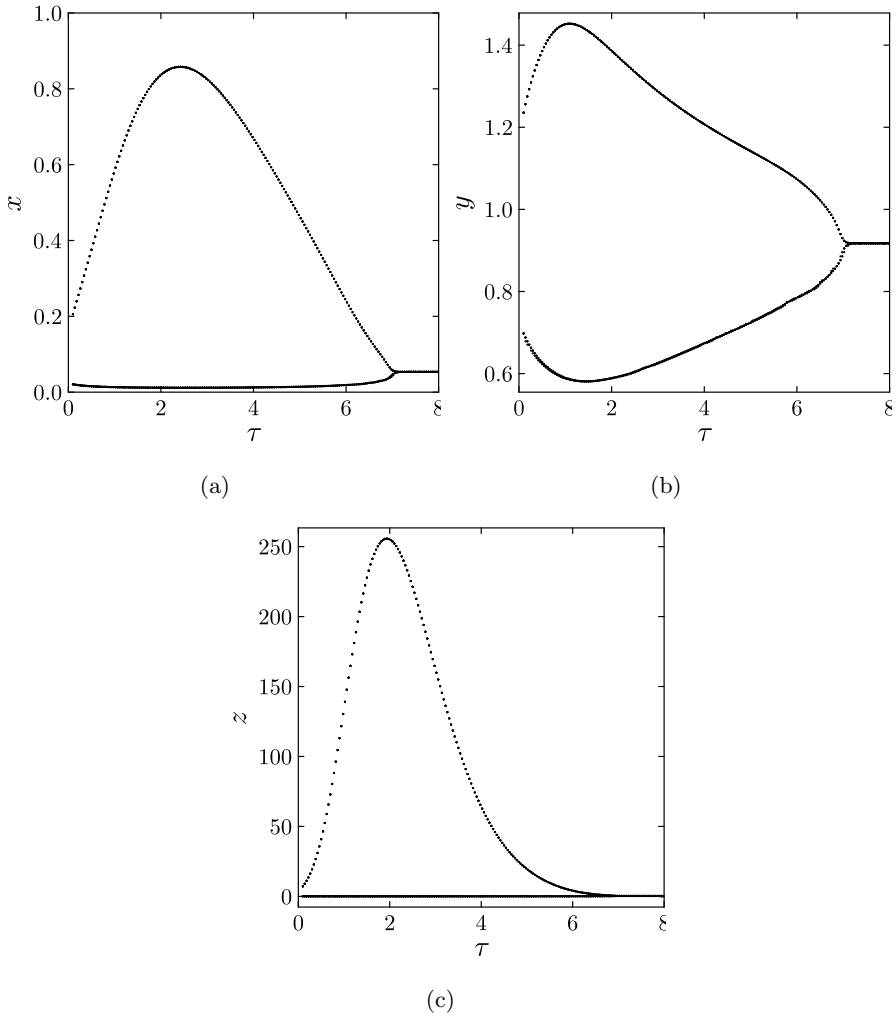

Fig. 12 (a) τ vs $x(t)$, (b) τ vs $y(t)$, & (c) τ vs $z(t)$; The bifurcation diagrams for the model (13) with $\tau \in (0,1)$, $\mu = 0.14$ and $k = 0.7$.

we proposed a mathematical model in this work to investigate the effect of fear and prey refuge on an intraguild predation model with gestation delay. It is reasonable to anticipate that the size of the prey will expand logistically when there are no predators present, and that the link between the prey and the predator will follow a ratio-dependent functional response [9]. First, we established the conditions for the existence of equilibrium points and explored the local asymptomatic behaviors of the proposed model surrounding them. This local dynamics of the model ensures the long term coexistence of populations. According to the results of our research, the suggested model exhibits Hopf-bifurcation when subjected to the impact of prey fear. Bifurcation analysis and population extinction, both essential for maintaining populations within the ecological system, were used to examine the model's complicated dynamical behavior [2, 40]. The model's periodic oscillations guarantee that its population size shows predictable, repeated cycles throughout time. Because of their inter-dependencies, the extinction of one species might put other species in danger or cause them to collapse. In the two-parameter plane, we determined the extinction zone by taking into account the effects of fear, prey refuge, catching, and conversion rate factors. This study aids in warning about possible population collapse or in implementing preventive measures. As a consequence of this, we arrived at the realization that both types of species reap benefits when prey numbers are allowed to remain below a specific threshold.

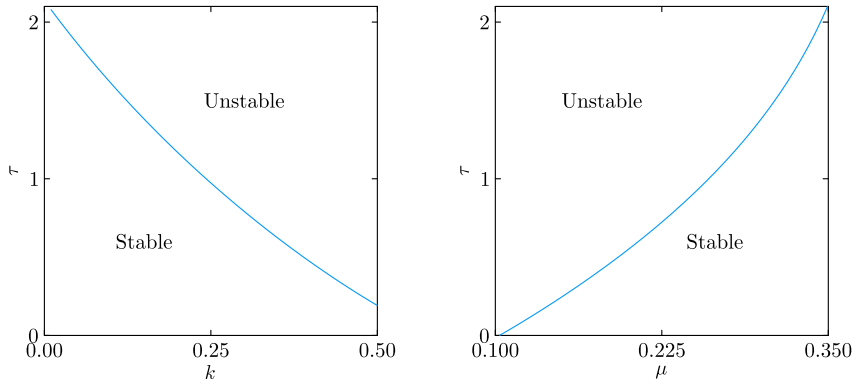

Fig. 13 (a) k vs τ & (b) μ vs τ; The two parameter bifurcation diagrams for the model (13) with different values of the model parameters. The blue line represents the Hopf curve which separates stable and periodic region.

In addition to this, we included the gestation delay of the predator population in the models that were suggested. After that, we looked at the suggested delayed model's local stability analysis as well as the possibility of Hopf bifurcation at an interior equilibrium point. We provided both numerical simulations and graphical representations to support the evidence that our analytical results revealed. Based on the results, we concluded that in both the suggested non-delayed and delayed models, the existence of fear, prey refuge, and delay has a major impact on stability transitions via Hopf-bifurcation.

We investigated a ratio-dependent intraguild predation model that accounted for fear effect, prey refuge, and gestation delay. Two prey populations and one predator population could be added to the model (2), which could have a massive effect on global biodiversity. It is explained how prey refuge and fear impact equilibrium levels. Our results shows that the stable-unstable-stable phenomena and other transition behavior show how sensitive the model's parameters are. When all species coexist, raising the prey refuge level has less of an impact on the population. In addition, variations in population size might be brought on by the predator's delayed gestation. Studying the dynamics of an intraguild predation model with additional functional responses may therefore be interesting and important. Exploring spatial dynamics remains an unexplored aspect, promising deeper insights into ecological dynamics. Additionally, incorporating different functional responses could enhance the model's understanding, contributing to the advancement of ecological modeling by opening new research aspects.

Appendix

Appendix A

In order to study the direction of the Hopf bifurcation and the stability of bifurcating periodic solution of model (13) at $\tau = \tau_0$. We followed the normal form method and center manifold theorem by Hassard et al. [34].

The Taylor expansion of the model (13) about the equilibrium point is

$$\begin{aligned}
\dot{x}(t) &= c_1x(t) + c_2y(t) + c_3z(t) + c_{11}x^2(t) + c_{12}x(t)y(t) + c_{13}x(t)z(t) + c_{14}y^2(t) + c_{15}y(t)z(t) + c_{16}z^2(t),\\
\dot{y}(t) &= c_4x(t-\tau) + c_5y(t) + c_6y(t-\tau) + c_7z(t) + c_{17}x^2(t-\tau) + c_{18}x(t-\tau)y(t-\tau)\\
&\quad + c_{19}y^2(t) + c_{20}y(t)z(t) + c_{21}y^2(t-\tau) + c_{22}z^2(t),
\end{aligned}$$

$$\dot{z}(t) = c_8x(t) + c_9y(t) + c_{10}z(t) + c_{23}x(t)z(t) + c_{24}y(t)z(t), \tag{A1}$$

where

$$c_{11} = -\frac{-r_1}{p(1+ky^*)z^*} + \frac{ny^{*2}\alpha(1-\mu)^2}{y^*+nx^*(1-\mu)}, c_{12} = \frac{-kr_1}{(1+ky^*)^2} + \frac{2kr_1x^*}{p(1+ky^*)^2z^*} + \frac{nx^*\alpha(1-\mu)^2}{(y+nx^*(1-\mu))^2},$$
$$-\frac{nx^*y^*\alpha(1-\mu)^2}{(y^*+nx^*(1-\mu))^3} + \frac{n^2x^{*2}\alpha(1-\mu)^3}{(y^*+nx^*(1-\mu))^3}, c_{13} = \frac{2r_1x^*}{p(1+ky^*)z^{*2}}, c_{14} = \frac{r_1k^2x^*}{(1+ky^*)^3}(1-\frac{x^*}{pz^*}),$$
$$+\frac{\alpha nx^{*2}(1-\mu)^2}{(y^*+nx^*(1-\mu))^2}, c_{15} = \frac{-kr_1x^{*2}}{p(1+ky^*)^2z^{*2}}, c_{16} = \frac{-r_1x^{*2}}{p(1+ky^*)z^{*3}}, c_{17} = \frac{-ny^{*2}\beta(1-\mu)^2}{(y^*+nx^*(1-\mu))^3},$$
$$c_{18} = \frac{n\beta x^*(1-\mu)^2}{(y^*+nx^*(1-\mu))^2} + \frac{nx^*y^*(1-\mu)^2}{(y^*+nx^*(1-\mu))^3} - \frac{n^2x^{*2}\beta(1-\mu)^3}{(y^*+nx^*(1-\mu))^3}, c_{19} = \frac{-r_2}{qz^*}, c_{20} = \frac{2r_2y^*}{qz^{*2}},$$
$$c_{21} = \frac{-nx^{*2}\beta(1-\mu)}{(y^*+nx^*(1-\mu))^3}, c_{22} = \frac{-r_2y^{*2}}{qz^{*2}}, c_{23} = -\delta, c_{24} = -\eta.$$

We can rewrite model (A1) as

$$\dot{x}(t) = L_\varphi + F(x_t, \varphi), \tag{A2}$$

where

$$L_\varphi(\phi) = B_1\phi(0) + B_2\phi(-\tau), \tag{A3}$$

and

$$F(\phi,\varphi) = \begin{pmatrix} c_{11}\phi_1^2(0) + c_{12}\phi(0)\phi_2(0) + c_{13}\phi_1(0)\phi_3(0) + c_{14}\phi_2^2(0) + c_{15}\phi_2(0)\phi_3(0) + c_{16}\phi_3^2(0) \\ c_{17}\phi_1^2(-\tau) + c_{18}\phi_1(-\tau)\phi_2(-\tau) + c_{19}\phi_2^2(0) + c_{20}\phi_2(0)\phi_3(0) + c_{21}\phi_2^2(-\tau) + c_{22}\phi_3^2(0) \\ c_{23}\phi_1(0)\phi_3(0) + c_{24}\phi_2(0)\phi_3(0) \end{pmatrix}, \tag{A4}$$

where

$$B_1 = \begin{pmatrix} c_1 & c_2 & c_3 \\ 0 & c_5 & c_7 \\ c_8 & c_9 * c_{10} & \end{pmatrix}, \quad B_2 = \begin{pmatrix} 0 & 0 & 0 \\ c_4 & c_6 & 0 \\ 0 & 0 & 0 \end{pmatrix}. \tag{A5}$$

Remaining steps are followed as in [33]. And we present some quantities required to find μ_2, β_2 and T_2.

Let $q(\theta) = Ve^{i\omega_0\theta}$ be eigenvector of A associated with $i\omega_0$, and $q^*(\theta) = DV^*e^{i\omega_0\theta}$ be eigenvector of A^* associated with $-i\omega_0$. Then

$$< q^*, q >= 1, \quad < q^*.\bar{q} >= 0, \tag{A6}$$

where $V = (1, \sigma_1, \sigma_2)^T, V^* = (1, \sigma_1^*, \sigma_2^*)^T$, and

$$\sigma_1 = \frac{c_2c_8 + (i\omega_0 - c_1)c_9}{c_2(i\omega_0 - c_{10}) + c_3c_9}, \sigma_2 = \frac{c_3c_7c_8 + (i\omega_0 - c_1)c_7c_9 + c_4e^{-i\omega_0\tau_0}(c_2(i\omega_0\tau_0 - c_{10}) + c_3c_9)}{(c_2(i\omega_0 - c_{10}) + c_3c_9)(i\omega_0 - c_5 - c_6e^{-i\omega_0\tau_0})},$$
$$\sigma_1^* = \frac{c_2c_8 - c_9(i\omega_0 + c_1)}{c_3c_9 - c_2(i\omega_0 + c_{10})}, \sigma_2^* = \frac{c_2c_7c_8 - c_7c_9(i\omega_0 + c_1) + c_4e^{i\omega_0\tau_0}(c_3c_9 - c_2(i\omega_0 + c_{10}))}{(c_3c_9 - c_2(i\omega_0 + c_{10}))(-i\omega_0 - c_5 - c_6e^{i\omega_0\tau_0})},$$
$$< q^*, q >= \bar{D}[1 + \bar{\sigma_1^*}\sigma_1 + \bar{\sigma_2^*}\sigma_2 + \tau_0e^{-i\omega_0\tau_0}(c_4\bar{\sigma_1^*} + c_6\sigma_1\bar{\sigma_1^*})],$$
$$\bar{D} = [1 + \bar{\sigma_1^*}\sigma_1 + \bar{\sigma_2^*}\sigma_2 + \tau_0e^{-i\omega_0\tau_0}(c_4\bar{\sigma_1^*} + c_6\sigma_1\bar{\sigma_1^*})]^{-1}.$$

Further, $\phi_i(0), \phi_i(-\tau)$, $i = 1,2,3$ are calculated as in [33]. And finally, we need the following values

$$E_1 = 2\begin{bmatrix} 2i\omega_0 - c_1 & -c_2 & -c_3 \\ -c_4e^{-2i\omega_0\tau_0} & 2i\omega_0 - c_5 - c_6e^{-2i\omega_0\tau_0} & -c_7 \\ -c_8 & -c_9 & 2i\omega_0 - c_{10} \end{bmatrix}^{-1} \begin{bmatrix} k_{11} \\ k_{21} \\ k_{31} \end{bmatrix}, \tag{A7}$$

$$E_2 = -\begin{bmatrix} c_1 & c_2 & c_3 \\ c_4 & c_5+c_6 & c_7 \\ c_8 & c_9 & c_{10} \end{bmatrix}^{-1} \begin{bmatrix} k_{12} \\ k_{22} \\ k_{32} \end{bmatrix}, \tag{A8}$$

where

$$\begin{aligned}
&k_{11} = c_{11} + c_{12}\sigma_1 + c_{13}\sigma_2 + c_{14}\sigma_1^2 + c_{15}\sigma_1\sigma_2 + c_{16}\sigma_2^2,\\
&k_{21} = c_{17}e^{-2i\omega_0\tau_0} + c_{18}e^{-2i\omega_0\tau_0} + c_{19}\sigma_1^2 + c_{20}\sigma_1\sigma_2 + c_{21}\sigma_1^2 e^{-2i\omega_0\tau_0} + c_{22}\sigma_2^2, k_{31} = c_{23}\sigma_2 + c_{24}\sigma_1\sigma_2,\\
&k_{12} = 2c_{11} + c_{12}(\sigma_1+\bar{\sigma_1}) + c_{13}(\sigma_2+\bar{\sigma_2}) + 2c_{14}\sigma_1\bar{\sigma_1} + c_{15}(\bar{\sigma_1}\sigma_2 + \sigma_1\bar{\sigma_2}) + 2c_{16}\sigma_2\bar{\sigma_2},\\
&k_{22} = 2c_{17} + c_{18}(\bar{\sigma_1}+\sigma_1) + 2c_{19}\sigma_1\bar{\sigma_1} + c_{20}(\bar{\sigma_1}\sigma_2 + \sigma_1\bar{\sigma_2}) + 2c_{21}\sigma_1\bar{\sigma_1} + 2c_{22}\sigma_2\bar{\sigma_2},\\
&k_{32} = c_{23}(\sigma_2+\bar{\sigma_2}) + c_{24}(\bar{\sigma_1}\sigma_2 + \sigma_1\bar{\sigma_2}).
\end{aligned}$$

and all other values are same as in [33].

Thus, we can compute the following quantities

$$\begin{cases}
\hat{c}_1(0) = \dfrac{i}{2\omega_0}(g_{20}g_{11} - 2|g_{11}|^2 - \dfrac{|g_{02}|^2}{3}) + \dfrac{g_{21}}{2},\\
\mu_2 = -\dfrac{\mathrm{Re}\{\hat{c}_1(0)\}}{\mathrm{Re}\{\lambda'(\tau_0)\}},\\
\beta_2 = 2\mathrm{Re}\{\hat{c}_1(0)\},\\
T_2 = -\dfrac{\mathrm{Im}\{\hat{c_1}(0)\} + \mu_2\mathrm{Im}\{\lambda'(\tau_0)\}}{\omega_0}.
\end{cases} \tag{A9}$$

Acknowledgements

The corresponding author would like to thank SRM IST, Ramapuram, India, for their financial support, vide number SRM/IST-RMP/RI/004. Moreover, the authors are very much grateful to the anonymous reviewers and the editor Albert C.J. Luo for their constructive comments and valuable suggestions to improve the quality and presentation of the manuscript significantly.

References

[1] Malthus, T.R. (1999), An essay on the principle of population: an essay on the principle of population, as it affects the future improvement of society with remarks on the speculations of mr. godwin, m. condorcet, and other writers.
[2] Friedman, A. (2018), Mathematical biology, *American Mathematical Society*, **127**.
[3] Capone, F., Carfora, M.F., De Luca, R., and Torcicollo, I. (2018), On the dynamics of an intraguild predator-prey model, *Mathematics and Computers in Simulation*, **149**, 17-31.
[4] Ganguli, C., Kar, T., and Mondal, P. (2017), Optimal harvesting of a prey-predator model with variable carrying capacity, *International Journal of Biomathematics*, **10**(5), 1750069.
[5] Vinoth, S., Vadivel, R., Hu, N.T., Chen, C.S., and Gunasekaran, N. (2023), Bifurcation analysis in a harvested modified Leslie-Gower model incorporated with the fear factor and prey refuge, *Mathematics*, **11**(14), 3118.
[6] Tripathi, J.P., Abbas, S., and Thakur, M. (2015), A density dependent delayed predator-prey model with Beddington-Deangelis type function response incorporating a prey refuge, *Communications in Nonlinear Science and Numerical Simulation*, **22**(1-3), 427-450.
[7] Shi, X., Zhou, X., and Song, X. (2011), Analysis of a stage-structured predator-prey model with Crowley-Martin function, *Journal of Applied Mathematics and Computing*, **36**(1-2), 459-472.
[8] Tripathi, J.P., Tyagi, S., and Abbas, S. (2016), Global analysis of a delayed density dependent predator-prey model with Crowley-Martin functional response, *Communications in Nonlinear Science and Numerical Simulation*, **30**(1-3), 45-69.
[9] Arditi, R. and Ginzburg, L.R. (1989), Coupling in predator-prey dynamics: ratio-dependence, *Journal of Theoretical Biology*, **139**(3), 311-326.

[10] Panja, P., Jana, S., and Mondal, S. (2021), Dynamics of a stage structure prey-predator model with ratio-dependent functional response and anti-predator behavior of adult prey, *Numerical Algebra, Control and Optimization*, **11**(3), 391.
[11] Magudeeswaran, S., Sathiyanathan, K., Sivasamy, R., Vinoth, S., and Sivabalan, M. (2021), Analysis on dynamics of delayed intraguild predation model with ratio-dependent functional response, *Discontinuity, Nonlinearity, and Complexity*, **10**(3), 381-396.
[12] Jiang, X., Zhang, R., and She, Z. (2021), Dynamics of a diffusive predator-prey system with ratio-dependent functional response and time delay, *International Journal of Biomathematics*, **13**(6), 2050036.
[13] Flores, J.D. and González-Olivares, E. (2014), Dynamics of a predator-prey model with Allee effect on prey and ratio-dependent functional response, *Ecological Complexity*, **18**, 59-66.
[14] Cannon, W.B. (1915), Bodily changes in pain, hunger, fear, and rage.
[15] Wang, X., Zanette, L., and Zou, X. (2016), Modelling the fear effect in predator-prey interactions, *Journal of Mathematical Biology*, **73**(5), 1179-1204.
[16] Hossain, M., Pal, N., Samanta, S., and Chattopadhyay, J. (2020), Fear induced stabilization in an intraguild predation model, *International Journal of Bifurcation and Chaos*, **30**(4), 2050053.
[17] Devi, S. (2013), Effects of prey refuge on a ratio-dependent predator-prey model with stage-structure of prey population, *Applied Mathematical Modelling*, **37**(6), 4337-4349.
[18] Chakraborty, S., Tiwari, P.K., Sasmal, S.K., Biswas, S., Bhattacharya, S., and Chattopadhyay, J. (2017), Interactive effects of prey refuge and additional food for predator in a diffusive predator-prey system, *Applied Mathematical Modelling*, **47**, 128-140.
[19] Lv, Y., Zhang, Z., Yuan, R., and Pei, Y. (2014), Effect of harvesting and prey refuge in a prey-predator system, *Journal of Biological Systems*, **22**(1), 133-150.
[20] Barman, D., Roy, J., Alrabaiah, H., Panja, P., Mondal, S.P., and Alam, S. (2021), Impact of predator incited fear and prey refuge in a fractional order prey predator model, *Chaos, Solitons and Fractals*, **142**, 110420.
[21] Panja, P. (2021), Combine effects of square root functional response and prey refuge on predator-prey dynamics, *International Journal of Modelling and Simulation*, **41**(6), 426-433.
[22] Kar, T.K. (2004), Stability analysis of a prey-predator model with delay and harvesting, *Journal of Biological Systems*, **12**(1), 61-71.
[23] Song, Y., Yin, T., and Shu, H. (2017), Dynamics of a ratio-dependent stage-structured predator-prey model with delay, *Mathematical Methods in the Applied Sciences*, **40**(18), 6451-6467.
[24] Rihan, F., Lakshmanan, S., Hashish, A., Rakkiyappan, R., and Ahmed, E. (2015), Fractional order delayed predator-prey systems with Holling type-II functional response, *Nonlinear Dynamics*, **80**, 777-789.
[25] Jia, L. and Wang, C. (2020), Persistence of a Lotka-Volterra ratio-dependent predator-prey model with delays and feedback controls, *IOP Conference Series: Materials Science and Engineering*, **790**, 012129.
[26] Sk, N., Tiwari, P.K., and Pal, S. (2022), A delay nonautonomous model for the impacts of fear and refuge in a three species food chain model with hunting cooperation, *Mathematics and Computers in Simulation*, **192**, 136-166.
[27] Mondal, B., Roy, S., Ghosh, U., and Tiwari, P.K. (2022), A systematic study of autonomous and nonautonomous predator-prey models for the combined effects of fear, refuge, cooperation and harvesting, *The European Physical Journal Plus*, **137**(6), 724.
[28] Sk, N., Tiwari, P.K., Kang, Y., and Pal, S. (2021), A nonautonomous model for the interactive effects of fear, refuge and additional food in a prey-predator system, *Journal of Biological Systems*, **29**(1), 107-145.
[29] Magudeeswaran, S., Vinoth, S., Sathiyanathan, K., and Chaisena, K. (2023), Fear effect on a delayed intraguild predation model with the ratio-dependent functional response, *International Journal of Nonlinear Analysis and Applications*, **14**(1), 927-940.
[30] Xiao, D. and Ruan, S. (2001), Global dynamics of a ratio-dependent predator-prey system, *Journal of Mathematical Biology*, **43**, 268-290.
[31] Vinoth, S., Sivasamy, R., Sathiyanathan, K., Unyong, B., Rajchakit, G., Vadivel, R., and Gunasekaran, N. (2021), The dynamics of a Leslie type predator-prey model with fear and Allee effect, *Advances in Difference Equations*, **2021**, 1-22.
[32] Vinoth, S., Sivasamy, R., Sathiyanathan, K., Rajchakit, G., Hammachukiattikul, P., Vadivel, R., and Gunasekaran, N. (2021), Dynamical analysis of a delayed food chain model with additive Allee effect, *Advances in Difference Equations*, **2021**(1), 1-20.
[33] Meng, X.Y., Huo, H.F., and Xiang, H. (2011), Hopf bifurcation in a three-species system with delays, *Journal of Applied Mathematics and Computing*, **35**(1), 635-661.
[34] Hassard, B.D., Kazarinoff, N.D., and Wan, Y.H. (1981), Theory and applications of Hopf bifurcation, *Cambridge University Press Archive*, **41**.
[35] Kumar, V. and Kumari, N. (2020), Controlling chaos in three species food chain model with fear effect, *AIMS Mathematics*, **5**(2), 828.

[36] Panday, P., Pal, N., Samanta, S., and Chattopadhyay, J. (2018), Stability and bifurcation analysis of a three-species food chain model with fear, *International Journal of Bifurcation and Chaos*, **28**(1), 1850009.
[37] Khajanchi, S. and Banerjee, S. (2017), Role of constant prey refuge on stage structure predator-prey model with ratio dependent functional response, *Applied Mathematics and Computation*, **314**, 193-198.
[38] Doedel, E.J. (1981), AUTO: A program for the automatic bifurcation analysis of autonomous systems, *Congressus Numerantium*, **30**, 265-284.
[39] Ermentrout, B. and Mahajan, A. (2003), Simulating, analyzing, and animating dynamical systems: a guide to XPPAUT for researchers and students, *Applied Mechanics Reviews*, **56**(4), B53.
[40] Sen, D., Ghorai, S., Banerjee, M., and Morozov, A. (2022), Bifurcation analysis of the predator-prey model with the Allee effect in the predator, *Journal of Mathematical Biology*, **84**(1), 7.